



## OPEN ACCESS

## EDITED BY

Fei Xue,  
Hohai University, China

## REVIEWED BY

Teng Ding,  
Hohai University, China  
Hailong Huo,  
Chinese Academy of Geological  
Sciences (CAGS), China

## \*CORRESPONDENCE

Sen Wang,  
wangsen\_cug@163.com

## SPECIALTY SECTION

This article was submitted  
to Economic Geology,  
a section of the journal  
Frontiers in Earth Science

RECEIVED 25 August 2022

ACCEPTED 07 November 2022

PUBLISHED 26 January 2023

## CITATION

Wang S, Cao K, Zhang D, Yi J-J, Hu B-J, Yang J, Cai M-Y, Zhang Y-Y, Yuan Y and Pan T-W (2023). Mineralization age and genesis of the makeng-style iron deposits in the Paleo-Pacific tectonic domain of South China: *In situ* LA-ICPMS garnet U-Pb chronological and geochemical constraints. *Front. Earth Sci.* 10:1027620. doi: 10.3389/feart.2022.1027620

## COPYRIGHT

© 2023 Wang, Cao, Zhang, Yi, Hu, Yang, Cai, Zhang, Yuan and Pan. This is an open-access article distributed under the terms of the [Creative Commons Attribution License \(CC BY\)](#). The use, distribution or reproduction in other forums is permitted, provided the original author(s) and the copyright owner(s) are credited and that the original publication in this journal is cited, in accordance with accepted academic practice. No use, distribution or reproduction is permitted which does not comply with these terms.

# Mineralization age and genesis of the makeng-style iron deposits in the Paleo-Pacific tectonic domain of South China: *In situ* LA-ICPMS garnet U-Pb chronological and geochemical constraints

Sen Wang<sup>1,2,3\*</sup>, Ke Cao<sup>4</sup>, Da Zhang<sup>5</sup>, Jin-Jun Yi<sup>6</sup>, Bo-Jie Hu<sup>5</sup>, Jing Yang<sup>1,2,3</sup>, Meng-Ying Cai<sup>5</sup>, Yao-Yao Zhang<sup>5</sup>, Yuan Yuan<sup>5</sup> and Tian-Wang Pan<sup>5</sup>

<sup>1</sup>Institute of Geomechanics, Chinese Academy of Geological Sciences, Beijing, China, <sup>2</sup>Key Laboratory of Paleomagnetism and Tectonic Reconstruction, Ministry of Natural Resources, Beijing, China,

<sup>3</sup>Research Center of Polar Geosciences, China Geological Survey, Beijing, China, <sup>4</sup>Beijing Research Institute of Uranium Geology, Beijing, China, <sup>5</sup>China University of Geosciences (Beijing), Beijing, China,

<sup>6</sup>Cores and Samples Centre of Natural Resources, China Geological Survey, Sanhe, China

To reveal the genesis of Makeng-style iron polymetallic deposits from SE China in the paleo-Pacific tectonic domain, a new analytical method of LA-ICPMS garnet U-Pb dating and rare Earth element analysis was conducted for the Makeng, Luoyang, Dapai and Pantian deposits. The U-Pb dating results of nine garnet skarn samples from these deposits suggested that the Makeng-style iron polymetallic deposits mainly formed during 137–130 Ma, which is consistent with the zircon U-Pb and molybdenite Re-Os ages. This study provides more direct evidence of the mineralization age and the relationship between mineralization and granite, compared with previous studies on the zircon U-Pb dating for granites in the ore fields. Rare Earth element (REE) analysis results and REE patterns of four representative garnet samples from the Makeng, Luoyang, Dapai and Pantian deposits show that they are similar to typical skarn deposits, but obvious differences in the REE distribution types indicate that the ore-forming process may be distinct due to different mineralizing fluid for these Makeng-style deposits. Our new garnet U-Pb dating and rare Earth element analysis result not only provides new evidence for the mineralization age and genesis of the Makeng-style deposits but is also of great significance to promote the application of U-Pb dating methods to research skarn type deposits.

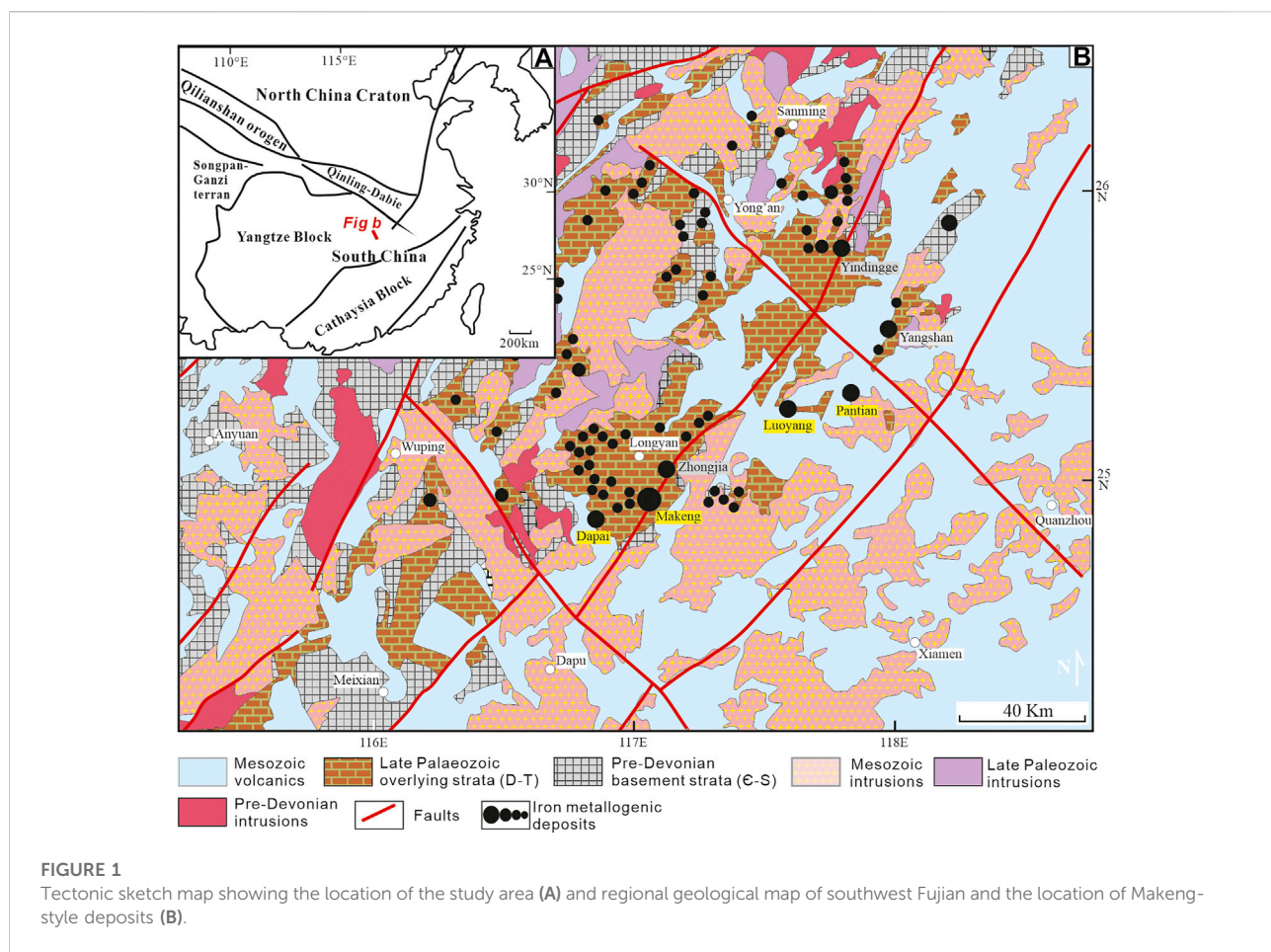
## KEYWORDS

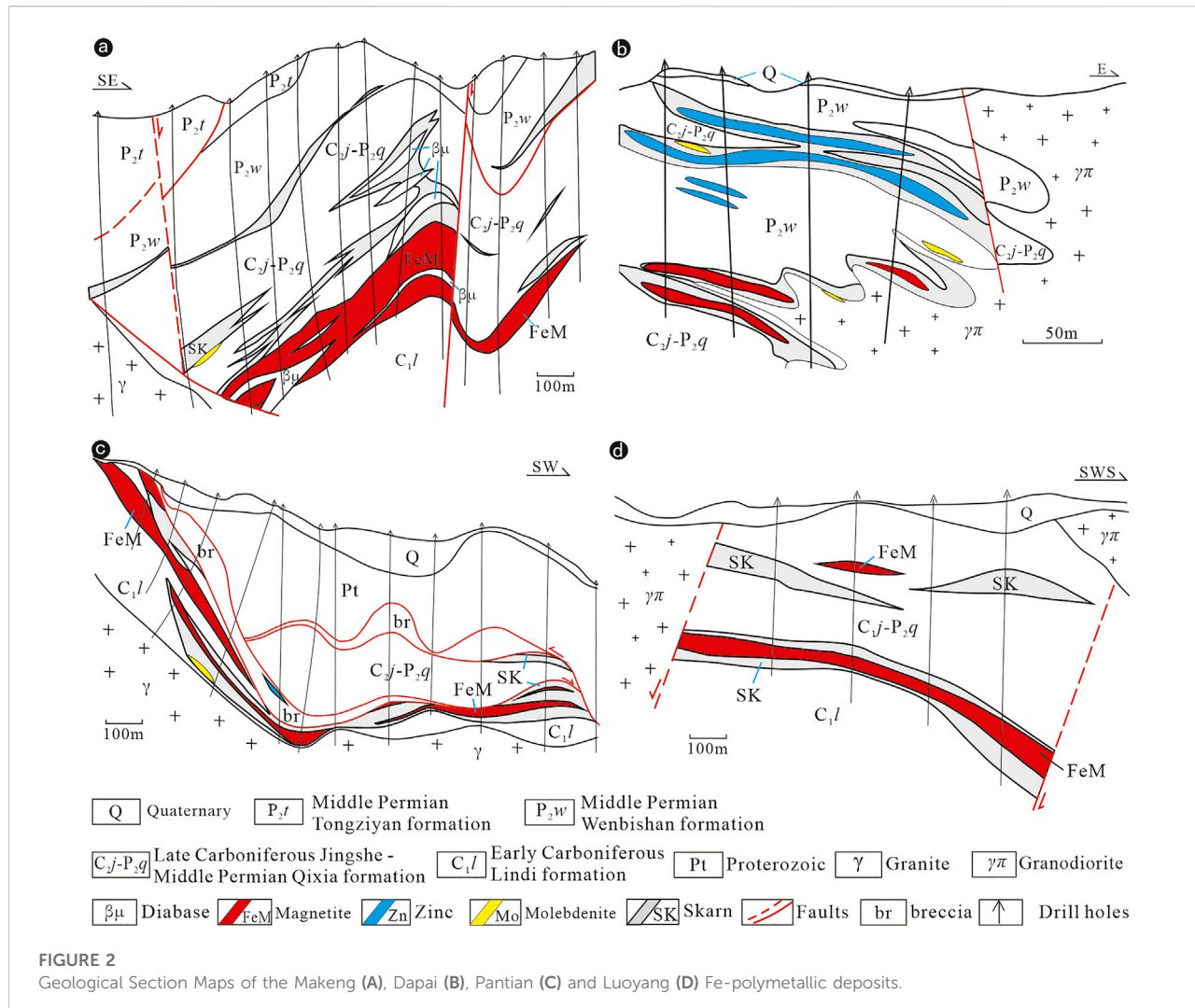
garnet U-Pb dating, ore genesis, makeng-type deposits, mineralization age, southwestern fujian

## Introduction

The Southwestern Fujian Iron Polymetallic Metallogenic Belt (SFIPMB) is one of the most important mineralization zones in the Southeast China Block of the paleo-Pacific tectonic domain (Figure 1A), and abundant iron deposits were hosted along this belt, such as the Makeng, Dapai, Pantian, Luoyang, Yangshan, Tangquan, and Zhongjia deposits (Figure 1B). These deposits are typically referred to as “Makeng-style iron deposits” due to their spatial and genetic association with the super large scale Makeng iron polymetallic deposit (Zhang et al., 2018a; Wang et al., 2018a; Wang et al., 2021). These deposits have similar metallogenic characteristics, and ore bodies are usually found between the early Carboniferous siliceous clastic rocks and late Carboniferous - middle Permian limestones with stratiform or stratoid shapes and large sizes. Many studies have been performed on the genesis of Makeng-style iron polymetallic deposits (Han and Ge, 1983; Zhang et al., 2018a; Zhang et al., 2013; Zhang and Zhang, 2014; Zhang and Zuo, 2014; Zhang et al., 2015; Wang et al., 2017a; Yang et al., 2017; Wang et al., 2018a), but controversy remain due to different understanding on the mineralization age. Some scholars held on the idea that the mineralization of the

Makeng-style iron deposit was related to Early Cretaceous granites (ca. 135–130 Ma, Zhang et al., 2018a; Zhang et al., 2013; Zhang et al., 2018a). However, other scholars put forward different opinions on the mineralization age according to the relationship between the magnetite orebodies and other wall rocks, and provided chronological evidences of 160–150 Ma (Wang et al., 2010; Yan, 2013; Zhang et al., 2015; Wang et al., 2017a). Especially in the last few years, zircon U-Pb ages of 160–150 Ma for granites from these Makeng-style deposits were reported, such as  $154.9 \pm 0.9$  Ma for Makeng deposit (Yan, 2013),  $152.7 \pm 1.4$  Ma for the Luoyang deposit (Yu, 2017), and  $150.2 \pm 0.5$  Ma for Dapai deposit (Yuan et al., 2020). Together with garnet Sm-Nd ages ( $157 \pm 15$  Ma, Zhang et al., 2015), zircon U-Pb ages of granites and basic rocks suggested that the mineralization may occur at 160–150 Ma (Yan, 2013; Zhang et al., 2015; Wang et al., 2017a; Yu, 2017; Yuan et al., 2020). To sum up, there are two main viewpoints on the mineralization age for the Makeng-style deposits due to different research objects and analytical methods they selected. In addition, different understandings on the mineralization age further affects explanations of the ore genesis, and therefore, the controversy on the mineralization age for the Makeng-style





deposits needs to be solved urgently. Garnet-magnetite and diopside-magnetite are the major ore types with massive and banded structures for these Makeng-style deposits. The garnets are mainly andradites and closely associated with the magnetites in space. These garnets usually have good crystal shapes, and they are accompanied by xenomorphic magnetites. At present, it is impossible to carry out direct dating on magnetites, and therefore, the dating research on garnets can provide more direct constraints on the mineralization age due to their close spatial relationship with magnetites. Along with the development of laser ablation inductively coupled plasma-mass spectrometry (LA-ICPMS), *in-situ* garnet U-Pb isotope analysis has been gradually realized (Chen et al., 2016; Deng et al., 2017; Seman et al., 2017; Tang et al., 2021). As a main kind of skarn mineral, garnet has been used in dating research the skarn type deposits and yields accurate U-Pb ages (Deng et al., 2017; Li et al., 2018; Wafforn et al., 2018; Stifeeva et al., 2019; Duan et al., 2020; Tang et al., 2021). In this paper, ore-bearing skarns were selected from

the Makeng, Luoyang, Dapai and Pantian deposits to carry out garnet U-Pb dating and rare Earth element analysis research and provide new evidence on the mineralization age and ore genesis for the Makeng-style iron polymetallic deposits. This research not only provides new chronology and geochemical evidence for the generation of the Makeng-style deposits but is also of great significance to promote the application of new U-Pb dating methods to the study of skarn type deposits.

## Regional geological setting

The global tectonic pattern underwent some major changes with frequent magmatic-polymetallic mineralization in eastern China during the Yanshanian period. Located in the eastern part of the South China Plate, the southwestern Fujian area has been affected by the subduction of the Pacific Plate since the Mesozoic and Cenozoic, and the metallogenic domains of the circum-

Pacific have occurred with large-scale copper, molybdenum, iron, gold silver, lead and zinc mineralization, such as the Zijinshan copper-gold deposit and Makeng iron deposit.

Located on the western margin of the Paleo-Pacific tectonic domain, the Makeng-style deposits are important iron polymetallic ore deposits in the SE China. These iron polymetallic ores are controlled by regional structures with an obvious NE-trending distribution (Figure 1). Sedimentary rocks distributed in the metallogenic belt are mainly.

The following three types in general: pre-Devonian basement rocks, late Paleozoic-middle Triassic clastic sedimentary and cap carbonate strata, and Mesozoic continental clastic and volcanic rocks (Wang et al., 2017b). Among these rocks, Early Carboniferous siliceous clastic rocks and Late Carboniferous - middle Permian limestones are most closely related to the iron polymetallic ore bodies in space (Figure 2). The iron polymetallic metallogenic belt is a most important part of the Mesozoic tectonic-magmatic zone on the west side of the Pacific plate. Mesozoic acidic and intermediate-acidic magmatic rocks are widely developed in the ore districts of Makeng-style deposits, with U-Pb ages mainly ranging from 135 to 130 and 160 to 150 (Wang et al., 2015). These intrusive rocks are closely related to the magnetite ore bodies in space, but there is a lack of direct evidence for the relationship between them. The iron orebodies mainly occurred in the garnet skarn and obviously controlled by strata, not in the contact zone of the granites. The Makeng-style iron polymetallic deposits are accompanied by Mo-, Pb- and Zn-bearing minerals, and previous studies have demonstrated that the molybdenite formed during 135–130 Ma (Zhang et al., 2018a; Zhang et al., 2012b); however, unlike the magnetites, molybdenites were only found within the granite bodies and in the fracture surface of wall rocks and iron ores. Therefore, there is no direct evidence to suggest that the molybdenite is contemporaneous with magnetite. The Early Cretaceous granites are the major magmatic rocks in the SFIPMB (Figure 2), and they are most likely metallogenic rocks; however, there is no direct evidence to verify that the iron mineralization is related to the Cretaceous granite, especially for the Makeng deposit.

## Ore features

As one of the most important super large iron deposits in South China, the Makeng iron polymetallic deposit was taken as an example to display its ore features in this paper. The Makeng iron deposit is characterized by thick and large single orebody with a maximum thickness of >50 m (>200 m in the Makeng deposit), but it shows remarkable variations in different positions due to the control of folds and faults. The main ore bodies formed in the contact zone between the Early Carboniferous clastic rocks

(C<sub>1</sub>I) and Late Carboniferous-Middle Permian carbonate rocks (C<sub>2</sub>j-P<sub>2</sub>q) with bedded and para-bedded shapes. Magnetite is the major metal-bearing mineral in these deposits, with some hematite, pyrite, molybdenite and sphalerite. As a kind of later hydrothermal modified mineral, molybdenite is often filled in the fracture surface of wall rocks and iron ores with vein and scattered shapes. Garnet and diopside is the primary gangue minerals and they are closely associated with the iron-rich ores. The garnet associated with magnetite is reddish brown and dark in color, which has typical characteristics of andradite garnet. In addition, vein magnetite is often observed in the mineralized bodies, and they are always accompanied by skarn minerals. The iron ores mainly show semi-euhedral to euhedral medium—coarse granular texture, with a small amount of metasomatic texture. Dense massive structure is the most important ore structure in the Makeng deposit, accounting for more than 70%. Skarn is the most important alteration type in this deposit. Associated with magnetites, the garnet and diopside accounted for a vast majority of the altered minerals. Despite it has large size of iron ore bodies and the wide variety of skarn minerals, there is no obvious zonation of skarn observed in the mine.

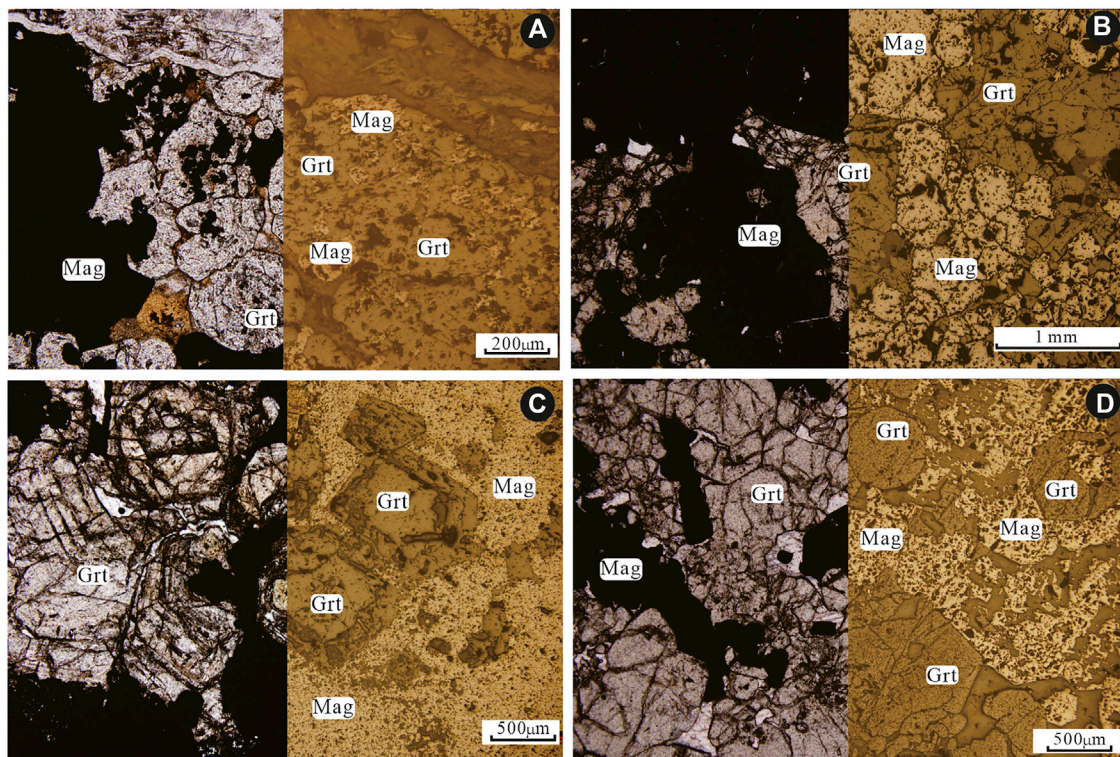
## Sampling and analytical methods

### Sample description

Samples of garnet skarn collected from the Makeng, Luoyang, Dapai and Pantian deposits were selected to carry out LA-ICPMS garnet U-Pb dating in this paper. A total of nine samples were collected from the mine channel and drill holes of the Makeng (102-2-b4, 108-1-b6, ZK7525-b1, and 214-b9), Luoyang (ZK405-b13 and BL23), Dapai (ZK403-b92 and ZK403-b67), and Pantian (PTPD-b1) iron polymetallic ore deposits. These samples were collected from the ore-bearing garnet skarn in different deposits and different orebodies of a same deposit. The garnets were concomitant with magnetites in these selected samples. Magnetite was the main ore mineral with little pyrite, pyrrhotite and chalcopyrite, along with garnet as major gangue mineral. Micrographs of representative samples showed that garnet was formed with good crystal morphology and closely association with magnetite in space (Figure 3). The garnets have euhedral and semi-euhedral granular textures with crystal size ranging from 200 to 500 μm, with typical growth bands developed locally.

### Analytical method

These spots with no cracks and inclusions were selected from each thin section of these samples to carry out the experiment. Garnet U-Pb dating and rare element analysis was performed using a GeoLasHD ArF laser ablation (LA) and an Agilent

**FIGURE 3**

Microphtographs showing the accompanying relationship between garnets and Magnetites from Makeng (A), Luoyang (B) Dapai (C) and Pantian (D) deposits. (The left photos are cross-polarized light; the right photos are plane-polarized light). Gr—Garnet; Mag—Magnetite.

**TABLE 1** Major parameters for the garnet LA-ICP-MS U-Pb dating method.

#### La ablation (GeoLasHD 193 nm ArF)

Energy density	5 mJ/cm <sup>2</sup>
Ablation frequency	5 Hz
Sampling time	50 s
Spot beam diameter	90 μm
Carrier gas type	He
Flow rate of carrier gas	0.4 L/min

#### Inductively Coupled Plasma Mass Spectrometer (Agilent 7900)

Plasma flow (Ar)	15 L/min
RF power	1550 W
Sample depth	6.0 mm
Nebulizer gas	0.7–0.9 L/min
Analyzed Isotopes	204 Pb, 206 Pb, 207 Pb, 208 Pb, 232Th, and 238U
Integral time	25 ms/isotope

7900 inductively coupled plasma mass spectrometer (ICP-MS) at the Key Laboratory of Paleomagnetism and Tectonic Reconstruction, Ministry of Natural Resources, Beijing, China. A detailed introduction to the instrumental conditions was described in Wang et al. (2022). A spot beam size of 90 μm was used during the analysis, and the garnet Willsboro (Semant et al., 2017) was used as an external standard to test the isotope ratios of the samples. Detailed instrument parameters and analytical methods were listed in Table 1. After the analyses, ICPMSDataCal software (version 10.9) was applied to calculate the  $^{207}\text{Pb}/^{206}\text{Pb}$ ,  $^{206}\text{Pb}/^{238}\text{U}$ ,  $^{207}\text{Pb}/^{235}\text{U}$  and  $^{208}\text{Pb}/^{232}\text{Th}$  ratios (Liu et al., 2010). Tera-Wasserburg lower intercept ages were calculated using ISOPLOT 3.0 with quotes at the  $1\sigma$  and 95% confidence levels (Ludwig, 2003).

The experimental conditions and instrument parameters for *in-situ* rare Earth element analysis were the same as those for U-Pb dating, and it was done at the same time as U-Pb isotope analysis. The synthetic glass samples NIST 610 and NIST 612 were used as external standards to test the rare Earth element contents. ICPMSDataCal software (version 10.9) was applied to calculate the trace element contents (Liu et al., 2010).

TABLE 2 Rare Earth element analytical results ( $10^{-6}$ ) of garnets from the Makeng-style Fe-polymetallic deposits.

	La	Ce	Pr	Nd	Sm	Eu	Gd	Tb	Dy	Ho	Er	Tm	Yb	Lu	$\Sigma$ REE	$\Sigma$ LREE	$\Sigma$ HREE
<i>ZK7525-b1(Makeng)</i>																	
01	1.0511	6.9195	1.4148	6.5141	1.2001	1.4638	1.2303	0.1731	1.0909	0.1926	0.5554	0.0565	0.3849	0.0424	22.29	18.56	3.73
02	7.7441	16.1248	1.5024	4.5794	0.5664	1.5918	0.4048	0.0399	0.2755	0.0653	0.1418	0.0202	0.1294	0.0102	33.20	32.11	1.09
03	1.9392	10.6070	1.7749	7.3752	0.7531	1.1787	0.3680	0.0388	0.2796	0.0529	0.1255	0.0178	0.1281	0.0127	24.65	23.63	1.02
04	4.3721	21.6796	3.1853	10.9134	0.5770	2.1307	0.0981	0.0088	0.0749	0.0116	0.0398	0.0037	0.0328	0.0030	43.13	42.86	0.27
05	2.3394	13.8120	2.7234	13.5269	2.1568	2.0080	0.7899	0.0888	0.4821	0.0957	0.2481	0.0240	0.1882	0.0250	38.51	36.57	1.94
06	1.9611	12.7000	2.7739	14.3987	2.2763	2.0123	0.7815	0.0654	0.3577	0.0667	0.1652	0.0209	0.1188	0.0170	37.72	36.12	1.59
07	4.3600	10.8181	1.2398	4.0751	0.5735	1.0614	0.2687	0.0273	0.1407	0.0140	0.0468	0.0043	0.0244	0.0020	22.66	22.13	0.53
08	2.2326	10.5603	1.8081	7.4349	0.9926	1.8925	0.7205	0.0914	0.6364	0.1308	0.3517	0.0510	0.3070	0.0392	27.25	24.92	2.33
09	1.4338	12.5633	2.7543	12.2188	1.3476	1.9096	0.8892	0.0915	0.5660	0.0948	0.2554	0.0301	0.2157	0.0265	34.40	32.23	2.17
10	1.5277	12.3138	2.5876	12.0579	1.4400	2.3044	0.9618	0.1098	0.6338	0.1066	0.2912	0.0408	0.2563	0.0321	34.66	32.23	2.43
11	5.8394	24.2897	3.8759	14.1335	1.0092	1.6410	0.6452	0.0667	0.4062	0.0734	0.1796	0.0235	0.1330	0.0164	52.33	50.79	1.54
12	5.5209	30.6717	5.3221	19.3850	1.6243	2.3132	0.9414	0.0868	0.4797	0.0861	0.2385	0.0326	0.1782	0.0256	66.91	64.84	2.07
13	1.4196	10.5001	2.2783	9.9149	1.3746	2.4626	1.0956	0.1468	0.9445	0.2041	0.6027	0.0710	0.4836	0.0624	31.56	27.95	3.61
14	4.5438	25.1296	4.1587	15.5537	1.3910	2.0632	0.9133	0.0936	0.5490	0.1028	0.2785	0.0299	0.2113	0.0299	55.05	52.84	2.21
15	6.5024	32.8156	5.1419	18.0854	1.5075	2.0113	0.8631	0.0930	0.5877	0.1049	0.2540	0.0322	0.2244	0.0369	68.26	66.06	2.20
16	5.6732	26.1321	4.3100	15.9903	1.5073	1.8369	0.8971	0.1022	0.6701	0.1363	0.3596	0.0414	0.2457	0.0287	57.93	55.45	2.48
17	1.6416	12.1852	2.4598	10.4882	1.1855	2.5414	0.7662	0.0834	0.5293	0.0948	0.2766	0.0332	0.2260	0.0285	32.54	30.50	2.04
18	3.2099	14.1695	2.2996	8.3870	0.9917	2.1379	0.7278	0.0968	0.6288	0.1170	0.3305	0.0425	0.2848	0.0342	33.46	31.20	2.26
19	3.7863	15.8384	2.3186	8.0912	0.9939	2.0534	0.7337	0.0961	0.6300	0.1068	0.3005	0.0318	0.2483	0.0284	35.26	33.08	2.18
20	3.7038	9.2883	1.1049	3.5706	0.4840	0.4452	0.6994	0.1002	0.7451	0.1583	0.5056	0.0631	0.4328	0.0609	21.36	18.60	2.77
21	5.1273	24.5835	4.0859	15.2168	1.4227	1.7921	0.8538	0.1063	0.5707	0.1083	0.2771	0.0277	0.2370	0.0283	54.44	52.23	2.21
22	4.6833	24.0051	4.1259	15.8967	1.6407	1.9769	0.9464	0.1001	0.6607	0.1093	0.3323	0.0373	0.2478	0.0359	54.80	52.33	2.47
23	3.7407	11.5888	1.6581	5.9554	0.4976	0.8663	0.3709	0.0573	0.2710	0.0589	0.1474	0.0172	0.1362	0.0170	25.38	24.31	1.08
24	1.9029	7.4841	1.7470	7.1613	0.3856	1.3424	0.1337	0.0148	0.1026	0.0171	0.0549	0.0042	0.0445	0.0062	20.40	20.02	0.38
25	3.8681	12.2527	1.3884	4.1080	0.7592	0.6075	1.1233	0.1721	1.2859	0.2609	0.8491	0.0940	0.6128	0.0955	27.48	22.98	4.49
<i>ZK405-b13(Luoyang)</i>																	
01	1.6318	18.9420	3.6208	12.4251	1.3776	0.6372	1.2234	0.1610	1.1978	0.2327	0.7492	0.0922	0.6246	0.0896	43.00	38.63	4.37
02	2.5307	10.8800	1.8997	7.0440	0.7744	0.3625	0.8221	0.1068	0.8130	0.1650	0.5310	0.0549	0.3660	0.0587	26.41	23.49	2.92
03	1.1500	12.3946	3.2999	18.9805	3.4782	1.7076	2.1913	0.2622	1.6916	0.2997	0.9533	0.1278	0.9230	0.1325	47.59	41.01	6.58
04	2.7416	22.4241	3.4705	12.1399	1.2964	0.7525	1.0840	0.1144	0.7568	0.1699	0.5386	0.0659	0.4678	0.0714	46.09	42.82	3.27
05	3.1893	29.5146	4.6395	16.3949	2.2518	0.9138	1.6419	0.1702	1.2485	0.2539	0.6339	0.0796	0.5522	0.0734	61.56	56.90	4.65
06	2.8131	26.6198	4.0631	14.4076	1.3854	0.8251	0.9553	0.1156	0.8145	0.1630	0.4740	0.0599	0.3744	0.0457	53.12	50.11	3.00

(Continued on following page)

TABLE 2 (Continued) Rare Earth element analytical results ( $10^{-6}$ ) of garnets from the Makeng-style Fe-polymetallic deposits.

	La	Ce	Pr	Nd	Sm	Eu	Gd	Tb	Dy	Ho	Er	Tm	Yb	Lu	$\Sigma$ REE	$\Sigma$ LREE	$\Sigma$ HREE
07	2.6806	23.0889	3.3669	12.3883	1.4310	0.8080	1.0582	0.1205	0.8064	0.1478	0.4494	0.0514	0.3800	0.0429	46.82	43.76	3.06
08	3.6590	31.7782	5.0659	16.9251	2.0380	1.0113	1.5688	0.1805	1.2012	0.2314	0.6359	0.0706	0.4904	0.0686	64.92	60.48	4.45
09	2.9906	27.6522	4.6948	17.1033	2.1231	1.0702	1.6320	0.1873	1.1819	0.2237	0.6390	0.0768	0.4648	0.0765	60.12	55.63	4.48
10	2.2799	16.3760	2.5404	10.2058	1.3589	0.6961	1.1160	0.1321	0.8839	0.1837	0.4992	0.0611	0.3911	0.0530	36.78	33.46	3.32
11	1.9842	18.7467	3.5725	14.4271	1.3018	0.8764	0.9108	0.1001	0.7425	0.1478	0.4394	0.0541	0.3407	0.0393	43.68	40.91	2.77
12	2.0561	17.1829	3.1177	13.4685	1.9524	0.8579	1.1443	0.1463	0.8513	0.1791	0.4934	0.0618	0.4393	0.0529	42.00	38.64	3.37
13	1.3272	15.9018	3.5039	16.7142	2.7288	1.4957	1.7032	0.1811	1.1234	0.2061	0.5119	0.0670	0.5056	0.0730	46.04	41.67	4.37
14	1.9870	23.8286	4.9443	19.0179	1.9027	1.0655	1.2220	0.1386	0.8507	0.1693	0.5032	0.0655	0.4290	0.0570	56.18	52.75	3.44
15	1.6974	12.6234	2.3900	8.6535	0.9495	0.5565	0.8308	0.1084	0.7517	0.1801	0.5176	0.0700	0.4437	0.0540	29.83	26.87	2.96
16	2.3394	20.6711	4.4303	19.8793	2.2919	1.6971	1.6334	0.1996	1.1229	0.2179	0.6130	0.0677	0.6060	0.0704	55.84	51.31	4.53
17	2.5043	20.7491	4.5627	20.9617	2.4509	1.8231	1.6039	0.1881	1.2107	0.2346	0.7125	0.0773	0.6187	0.0758	57.77	53.05	4.72
18	1.6721	15.6917	3.5312	19.2296	2.5949	1.8019	1.5529	0.2048	1.1545	0.2379	0.5918	0.0774	0.5299	0.0784	48.95	44.52	4.43
19	2.2575	19.8059	4.4235	22.9732	2.9503	2.2468	1.7226	0.1830	1.0384	0.1736	0.5458	0.0597	0.4310	0.0560	58.87	54.66	4.21
20	1.0096	8.6143	2.2036	14.2014	2.4888	1.6490	1.4456	0.1484	0.9554	0.1591	0.4616	0.0527	0.4022	0.0524	33.84	30.17	3.68
21	1.5477	14.7754	3.7550	21.1765	3.2197	1.9556	2.2330	0.2134	1.2389	0.2062	0.5344	0.0598	0.3741	0.0538	51.34	46.43	4.91
22	1.0500	9.6963	2.4312	15.3127	2.4693	1.5986	1.5289	0.1463	0.7984	0.1434	0.4291	0.0420	0.3018	0.0427	35.99	32.56	3.43
23	1.5153	12.1859	2.6746	14.2925	2.2667	1.8449	1.3271	0.1256	0.8049	0.1267	0.3598	0.0386	0.2207	0.0339	37.82	34.78	3.04
24	1.5672	13.9509	3.4848	21.1427	3.5179	1.8598	2.4281	0.2796	1.6110	0.2859	0.8612	0.0870	0.6380	0.0858	51.80	45.52	6.28
25	2.3183	20.8837	4.5128	23.1011	3.1123	2.3469	1.9260	0.2016	1.2147	0.2266	0.5537	0.0675	0.4921	0.0554	61.01	56.28	4.74
26	1.7706	15.7116	4.0399	22.4558	3.7175	2.0435	2.3147	0.2569	1.4514	0.2688	0.6309	0.0776	0.5666	0.0853	55.39	49.74	5.65
27	1.5241	13.2116	3.0803	17.2316	2.5783	1.3475	1.8729	0.2164	1.3648	0.2383	0.7241	0.0803	0.6582	0.0703	44.20	38.97	5.23
28	1.9561	16.9369	3.8442	21.6208	3.2557	1.8414	2.1736	0.2408	1.4061	0.2790	0.7740	0.0823	0.6583	0.0887	55.16	49.46	5.70
29	2.0867	18.8196	4.7336	27.6026	3.7510	2.0496	2.4128	0.2489	1.4280	0.2750	0.7249	0.0846	0.5935	0.0716	64.88	59.04	5.84
30	1.0997	9.4070	2.4717	15.2702	2.8361	1.6101	1.7516	0.1890	1.1344	0.1895	0.5303	0.0679	0.4043	0.0571	37.02	32.69	4.32
31	1.3328	10.8895	2.5593	15.1774	2.9426	1.3439	2.2765	0.2557	1.7314	0.3027	0.7544	0.1069	0.6489	0.0803	40.40	34.25	6.16
32	2.2941	22.0588	5.0177	24.9277	3.1857	2.3627	2.4321	0.2846	1.6468	0.3411	0.9765	0.1116	0.8064	0.1139	66.56	59.85	6.71
	<i>ZK403-b67(Dapai)</i>																
01	18.5676	149.7086	24.8918	119.1647	25.5925	5.5164	21.2497	2.9471	17.7748	2.8081	7.4125	0.9392	6.7246	0.9317	404.23	343.44	60.79
02	13.7164	84.8239	13.3404	63.7800	15.9032	3.3963	16.0317	2.5336	16.3790	2.8714	8.2263	1.0606	8.1771	1.1976	251.44	194.96	56.48
03	19.9302	147.1071	26.2998	133.1006	30.3442	6.3753	24.5112	3.3014	20.3203	3.3324	8.7916	1.0685	7.7181	1.0178	433.22	363.16	70.06
04	21.5561	135.3794	19.7195	78.4955	14.2821	2.9630	11.3037	1.6736	10.8462	1.8543	5.3637	0.7171	5.7557	0.9602	310.87	272.40	38.47
05	22.6094	146.9015	19.7643	71.1965	12.8132	2.4104	8.8981	1.2342	7.1507	1.2583	3.2478	0.4676	3.5896	0.6306	302.17	275.70	26.48
06	10.4163	69.4935	12.0579	60.6923	21.8035	5.5561	30.9912	5.7637	41.4288	7.9139	22.8901	3.0051	21.8317	2.8535	316.70	180.02	136.68
07	6.5006	52.9525	10.8622	66.5356	29.9339	6.3153	42.6875	6.7155	43.7278	7.5586	20.9671	2.5982	18.1306	2.2773	317.76	173.10	144.66

(Continued on following page)

TABLE 2 (Continued) Rare Earth element analytical results ( $10^{-6}$ ) of garnets from the Makeng-style Fe-polymetallic deposits.

	La	Ce	Pr	Nd	Sm	Eu	Gd	Tb	Dy	Ho	Er	Tm	Yb	Lu	$\Sigma$ REE	$\Sigma$ LREE	$\Sigma$ HREE
08	8.2492	63.0378	11.0353	55.0853	17.4637	4.7145	20.0108	2.9897	17.4843	2.7007	6.8854	0.8046	5.3306	0.6999	216.49	159.59	56.91
09	8.9883	89.5815	16.2302	65.6549	12.6399	1.8628	14.3808	2.2937	15.0911	2.8584	8.2767	1.0587	8.1866	1.1272	248.23	194.96	53.27
10	8.1247	75.1676	18.5828	120.1977	44.2088	9.4458	55.5477	8.8890	54.0320	8.5230	21.1186	2.5130	16.4826	1.8071	444.64	275.73	168.91
11	4.1680	45.7377	11.1144	70.6844	33.7360	10.2825	38.7804	5.5886	32.3750	5.3092	13.8423	1.6789	11.9645	1.4005	286.66	175.72	110.94
12	14.0696	108.9676	19.4068	90.0510	15.8997	3.5855	11.8507	1.6980	10.4921	1.9101	5.3956	0.7315	5.0559	0.6855	289.80	251.98	37.82
13	14.8768	108.3804	17.0199	74.6314	13.0850	3.7308	9.4994	1.3083	7.8643	1.2949	3.3736	0.4268	3.0908	0.3904	258.97	231.72	27.25
14	11.3556	80.3302	12.5499	54.8846	14.5022	3.3162	17.6682	2.8869	19.4817	3.5216	9.6850	1.2726	8.9936	1.1793	241.63	176.94	64.69
15	15.9084	115.2267	19.6550	85.9887	19.5723	5.2849	22.7809	3.9570	26.9652	4.9329	14.7900	1.9058	13.2983	1.5703	351.84	261.64	90.20
16	8.5553	56.0627	12.9183	72.7570	31.2280	4.1640	44.5373	6.4971	33.9623	4.6973	10.6233	1.1534	7.4609	0.9006	295.52	185.69	109.83
17	19.4520	151.8294	25.7649	109.6677	23.9800	6.4696	25.6234	3.9784	23.7282	3.7748	9.6261	1.1244	7.3011	0.7992	413.12	337.16	75.96
18	16.2071	111.8097	20.3680	96.7396	23.5256	6.5582	22.4537	3.2160	18.7413	2.8578	7.0014	0.7713	5.2475	0.5941	336.09	275.21	60.88
19	23.8900	130.8813	21.1451	111.2794	45.0579	8.9812	60.4282	9.5094	56.6118	9.0306	22.6732	2.6545	18.6269	2.2643	523.03	341.23	181.80
20	12.0831	93.4766	16.6909	73.7938	22.3876	4.0885	22.8136	3.1909	17.1161	2.6214	6.6858	0.8250	5.5461	0.7690	282.09	222.52	59.57
21	18.0946	125.3588	19.9945	90.5357	21.9612	3.6869	16.7259	2.1196	11.7362	1.8704	5.0722	0.6339	4.5003	0.6571	322.95	279.63	43.32
22	14.2638	119.3521	24.7194	130.4673	28.3763	7.3833	23.9593	3.9553	26.6862	5.0473	15.3923	2.0461	15.6476	2.1463	419.44	324.56	94.88
23	27.1295	199.4180	34.6795	171.3148	34.6050	7.4103	20.5384	2.4036	13.6708	2.1496	5.8639	0.7589	5.7670	0.8251	526.53	474.56	51.98
24	9.7301	100.5082	22.1331	130.4838	35.0412	7.5390	34.3516	5.0471	30.9258	4.9991	12.9653	1.5924	11.6520	1.5574	408.53	305.44	103.09
25	9.1961	97.5050	24.9159	156.1901	43.6286	9.2681	44.5966	6.7840	41.5643	7.0233	18.7588	2.3335	17.2282	2.3871	481.38	340.70	140.68
26	9.7282	96.1372	22.6761	138.4134	36.5328	7.2238	28.5554	3.8666	23.1895	3.9320	10.6480	1.3927	10.5211	1.4818	394.30	310.71	83.59
	<i>PTPD-b1(Pantian)</i>																
01	6.3058	45.5843	8.0230	30.7870	5.3362	1.2981	4.9196	0.7883	4.8678	1.0397	3.3214	0.5157	4.1664	0.6003	117.55	97.33	20.22
02	22.3512	133.3816	16.7390	50.9776	8.3350	1.8368	8.7390	1.6002	11.5199	2.5636	8.4628	1.5953	11.1727	1.6390	280.91	233.62	47.29
03	7.4608	99.0428	23.8060	106.4404	22.7510	3.4912	20.8460	3.6718	24.1642	5.2232	15.6804	2.7145	20.4964	3.2533	359.04	262.99	96.05
04	7.4408	102.6949	21.6307	87.4132	19.7832	2.8736	18.5519	3.1569	20.3985	4.8428	14.2465	2.3364	19.3547	2.7915	327.52	241.84	85.68
05	10.4879	135.2963	24.2545	93.3241	18.7525	3.0873	15.7440	2.5207	14.9216	3.0587	8.6533	1.5196	11.4994	1.6790	344.80	285.20	59.60
06	9.8248	127.6298	26.6301	97.1864	16.3760	2.9649	13.0568	2.0624	11.8008	2.5271	7.4594	1.1876	9.8769	1.4278	330.01	280.61	49.40
07	9.3586	120.7242	23.0635	90.8147	20.5674	3.0758	19.2776	3.2766	20.5932	4.6146	13.5263	2.2445	17.2010	2.8073	351.15	267.60	83.54
08	7.9458	98.9252	20.3456	81.1135	19.4790	2.6929	19.9564	3.4173	23.2977	5.2051	15.7355	2.7661	20.8296	3.2826	324.99	230.50	94.49
09	11.1338	134.2343	24.3647	85.1230	16.2063	2.5787	12.3034	1.9986	12.3979	2.7270	7.9586	1.2855	10.1962	1.6371	324.15	273.64	50.50
10	21.8164	146.9816	30.7482	158.0526	13.5590	4.4101	4.9693	0.7740	5.0552	1.1068	3.2651	0.5376	4.3627	0.6637	396.30	375.57	20.73
11	8.4329	100.9965	20.9209	90.3626	21.4806	3.1773	19.8503	3.4544	22.6205	4.9886	13.8999	2.5011	18.6586	2.9563	334.30	245.37	88.93
12	12.3024	79.7952	12.2410	45.8204	9.9223	1.6452	9.7065	1.5795	9.7280	2.0911	6.4566	1.1253	8.2648	1.3012	201.98	161.73	40.25
13	7.4845	46.9549	7.7741	31.3827	5.5891	1.3315	4.9949	0.7266	4.5024	0.9247	2.8264	0.4965	3.7786	0.5386	119.31	100.52	18.79
14	6.4952	87.0313	20.3883	102.1250	27.9114	3.8984	22.5160	3.3706	19.4713	3.8379	10.7546	1.8508	13.3980	1.9994	325.05	247.85	77.20

(Continued on following page)

TABLE 2 (Continued) Rare Earth element analytical results ( $10^{-6}$ ) of garnets from the Makeng-style Fe-polymetallic deposits.

	La	Ce	Pr	Nd	Sm	Eu	Gd	Tb	Dy	Ho	Er	Tm	Yb	Lu	$\Sigma$ REE	$\Sigma$ HREE
15	11.7144	112.7933	215.060	1111.7169	34.5537	4.5668	32.7462	5.6857	35.8346	7.9833	23.0757	3.9930	31.2993	4.7864	442.26	296.85
16	11.7457	98.3608	16.9213	86.1467	23.4916	3.3077	16.7525	2.7928	15.4025	3.2594	9.1188	1.4689	11.5576	1.6895	302.02	239.97
17	35.5771	183.1398	17.2836	35.0713	4.3689	0.9204	3.3946	0.5543	4.0902	0.9300	2.9085	0.5559	4.2352	0.6350	293.43	276.16
18	13.7926	96.3972	18.5461	80.0898	7.3199	2.0818	3.2058	0.4923	3.5562	0.7200	2.2042	0.3436	2.6456	0.4530	231.85	218.23
19	8.4601	62.9767	10.3445	36.6332	5.1563	1.1925	3.9761	0.6046	3.7850	0.8828	2.5417	0.4390	2.8301	0.4904	140.31	124.76
20	58.2553	146.1940	11.7743	29.2120	5.8579	0.9499	7.0135	1.6399	12.8074	3.4517	10.9856	2.1551	15.3119	2.2481	307.86	252.24
21	6.1153	45.5799	8.6548	35.1030	6.7341	1.3370	5.4722	0.9654	6.0196	1.3766	4.2950	0.7112	5.0095	0.7813	128.15	103.52
22	7.3029	51.6917	8.7893	34.9098	5.9583	1.1541	4.7305	0.7094	4.5991	1.0450	3.0534	0.5169	3.5433	0.4795	128.48	109.81
23	7.3427	89.8233	19.0443	85.8071	20.6900	2.8808	18.1352	3.0233	18.5837	3.9962	11.5017	1.9785	14.5404	2.2834	299.63	225.59
																74.04

## Results

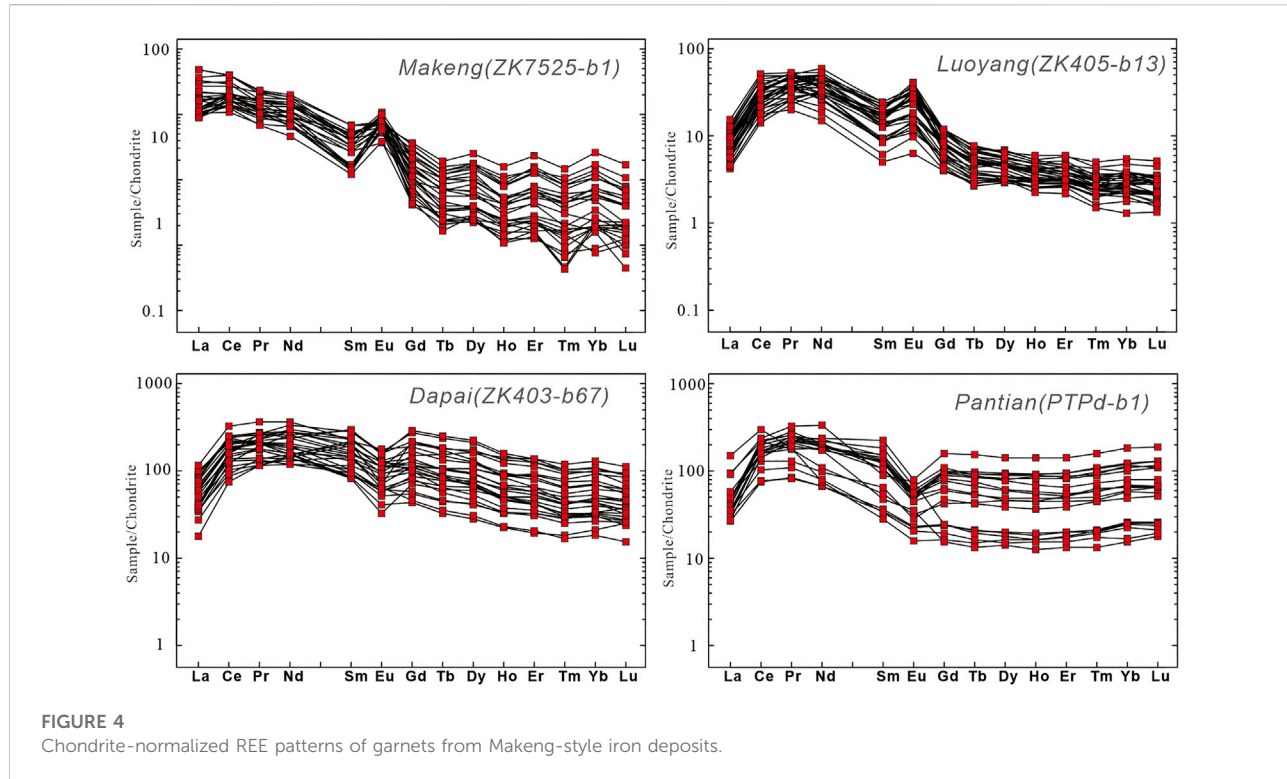
### Rare earth element analysis results

The rare Earth element analysis results are shown in [Table 2](#). A total of 25 and 32 spots of garnet sample ZK7525-b1 from the Makeng deposit and ZK405-b13 from the Luoyang deposit were selected to carry out rare Earth element analysis, respectively. Both of the two samples had lower REE contents with total REE contents ( $\Sigma$ REE) of 22.29–68.26 ppm (average value of 38.22 ppm) and 26.41–66.56 ppm (average value of 48.78 ppm), respectively. They were enrichment in light rare Earth elements with positive Eu anomalies. These samples showed right-sloping features in the chondrite-normalized REE patterns ([Figure 4](#)). Representative garnet sample ZK403-b67 and PTPD-b1 from Dapai and Pantian deposits had lower REE contents, with total REE contents ( $\Sigma$ REE) of 216.49–526.53 ppm ( $n = 26$ , average value = 349.14 ppm) and 117.55.41–396.30 ppm ( $n = 23$ , average value = 278.74 ppm), respectively. They showed flat REE distribution curves with weak negative Eu anomalies on the chondrite-normalized REE patterns ([Figure 4](#)).

### U-Pb dating results

The LA-ICPMS garnet U-Pb analysis results were listed in [Table 3](#). Four ore-bearing garnet samples (102-2-b1, 108-1-b6, ZK7525-b1, and 214-b9) were collected from different orebodies of the Makeng iron polymetallic deposit to analyze the U-Pb isotopic ratios. These spots of each sample showed good linear distribution features in the Tera-Wasserburg diagrams ([Figures 5A–D](#)). It yielded lower interception ages of  $133.3 \pm 2.5$  Ma,  $130.4 \pm 4.6$  Ma,  $132.6 \pm 3.5$  Ma and  $130.3 \pm 8.6$  Ma, respectively. A total of 17 and 28 spots were selected for two samples (ZK405-b13 and BL23) from the Luoyang deposit, which exhibited linear features on the Tera-Wasserburg diagram ([Figures 5E,F](#)) and yielded lower interception ages of  $137.5 \pm 3.7$  Ma and  $136.9 \pm 3.0$  Ma, respectively. A total of 25 and 30 spots were selected for two samples (ZK403-b92 and ZK403-b67) from the Dapai deposit, and it yielded lower interception ages of  $130.9 \pm 2.5$  Ma and  $132.1 \pm 2.0$  Ma respectively ([Figures 5G,H](#)). A total of 26 spots were selected for sample PTPD-b1 collected from the Pantian deposit, yielding a lower interception age of  $133.8 \pm 3.3$  Ma. Although these spots did not show a good linear feature, they were located near the concordant curve ([Figure 5I](#)), and therefore the lower interception age can represent the forming time of the garnet.

From a general view, the U-Pb ages of garnet skarn from the Makeng-style deposits are close with relatively concentrated ages ranging from 137 Ma to 130 Ma.



## Discussion

### Mineralization age

Dating the mineralization age is an important part in the ore genesis research, and the uncertainty of mineralization age will affect our understanding on the ore genesis. Due to the controversy on the mineralization age, there has been different understanding on the generation of the Makeng-style deposits, such as the sedimentary modified genesis and magmatic-hydrothermal genesis hypothesis (Han and Ge, 1983; Chen et al., 1985; Zhang et al., 2012b; Zhang et al., 2013; Wang et al., 2021). Previous research on the Makeng-style deposits mainly concentrated on zircon U-Pb dating for granites and Re-Os dating for molybdenites in ore districts (Zhang et al., 2018a; Zhang et al., 2012b; Lai et al., 2014; Yuan et al., 2014; Zhang et al., 2015; Zhao et al., 2016; Wang et al., 2018b), but the molybdenites were usually found in the interior of granite bodies and the fracture surface of the iron ores. Thus far, there is still no strongly evidence to prove that the magnetite mineralization is related to the intrusive rocks, or the magnetite are simultaneous with the molybdenites because they are not associated in space.

The ore-bearing garnet skarn rocks were selected to carry out LA-ICPMS garnet U-Pb dating, which can more directly constrain the mineralization age of the Makeng-style deposits

because the garnet was always concomitant with the magnetite in space. Four representative ore-bearing garnet samples from different orebodies of the Makeng deposit yielded lower interception ages of  $133.3 \pm 2.5$  and  $130.4 \pm 4.6$  Ma,  $132.6 \pm 3.5$  Ma and  $130.0 \pm 8.6$  Ma, respectively. These garnet U-Pb ages were close to each other and consistent with the zircon U-Pb dating results reported by Zhang et al. ( $129.6 \pm 0.8$  and  $132.6 \pm 1.3$  Ma, Zhang et al., 2012b) and Wang et al. ( $132.0 \pm 0.6$  Ma and  $132.4 \pm 0.8$ , Wang et al., 2015). In addition, the garnet and zircon U-Pb ages are close to the molybdenite Re-Os dating results with model ages ranging from  $131.9 \pm 1.9$  to  $133.3 \pm 2.3$  Ma (Zhang et al., 2012b).

To determine if the ore-forming ages were consistent among different deposits, five representative ore-bearing garnet samples from Luoyang, Dapai and Pantian were selected for U-Pb dating and yielded similar U-Pb ages. Two garnet samples from the Luoyang deposit yielded lower interception ages of  $137.5 \pm 3.7$  Ma and  $136.9 \pm 3.0$  Ma respectively, which are close to the zircon U-Pb ages of  $137.2 \pm 2.3$  Ma (Zhang et al., 2018b) and  $131.6 \pm 0.6$  Ma (Wang et al., 2021), and the molybdenite Re-Os ages of  $133.0 \pm 1.9$  Ma,  $133.1 \pm 1.9$  Ma and  $134.0 \pm 4.2$  Ma (Zhang et al., 2012b). Two samples selected from the Dapai deposit yielded lower interception ages of  $130.9 \pm 2.5$  Ma and  $132.1 \pm 2.0$  Ma respectively, which were consistent with the zircon U-Pb ages of  $132.4 \pm 0.8$  Ma (Yuan et al., 2020) and molybdenite Re-Os age of  $133.5 \pm 4.1$  Ma (Zhao et al., 2016). One sample collected

TABLE 3 LA-ICPMS garnet U-Pb data for skarn rocks from the Makeng-style iron polymetallic deposits.

Spot	U	Th	207Pb/ 206 Pb		207 Pb/235U		206 Pb/238U		207Pb/206 Pb		207 Pb/235U		206 Pb/238U	
			ppm	ppm	Ratio	1σ	Ratio	1σ	Ratio	1σ	Age (Ma)	1σ	Age (Ma)	1σ
<b>102-2-b4 (Makeng)</b>														
1	0.83	13.83	0.3148	0.0185	1.2978	0.0613	0.0330	0.0006	3546	90	845	27	209	4
2	0.13	0.76	0.7083	0.0440	21.1907	0.9921	0.2433	0.0076	-	-	3147	45	1404	39
3	1.52	67.71	0.1075	0.0053	0.3077	0.0121	0.0226	0.0004	1767	95	272	9	144	3
4	3.41	52.52	0.1149	0.0069	0.3438	0.0180	0.0234	0.0005	1880	108	300	14	149	3
5	0.03	7.50	0.1008	0.0083	0.2880	0.0208	0.0217	0.0005	1640	154	257	16	138	3
6	0.26	8.69	0.0601	0.0050	0.1856	0.0120	0.0218	0.0005	606	180	173	10	139	3
7	0.28	4.93	0.1844	0.0187	0.5900	0.0477	0.0260	0.0012	2694	168	471	30	165	7
8	0.71	68.47	0.0487	0.0027	0.1372	0.0072	0.0211	0.0004	132	126	131	6	134	2
9	0.16	42.26	0.0508	0.0028	0.1498	0.0074	0.0221	0.0003	232	126	142	7	141	2
10	0.11	35.00	0.0587	0.0028	0.1728	0.0074	0.0222	0.0003	567	101	162	6	142	2
11	0.11	13.08	0.0627	0.0045	0.1948	0.0122	0.0223	0.0005	698	152	181	10	142	3
12	0.09	11.95	0.0689	0.0054	0.2076	0.0141	0.0223	0.0005	896	161	192	12	142	3
13	0.05	9.47	0.0806	0.0059	0.2489	0.0177	0.0223	0.0005	1213	144	226	14	142	3
14	0.68	2.99	0.4757	0.0263	2.9812	0.1656	0.0482	0.0015	4168	82	1403	42	303	9
15	0.44	6.59	0.2992	0.0215	1.2300	0.0866	0.0320	0.0010	3466	112	814	39	203	7
16	0.40	4.40	0.2412	0.0164	0.8493	0.0518	0.0276	0.0007	3127	108	624	28	176	5
17	0.05	8.72	0.1261	0.0089	0.3721	0.0239	0.0230	0.0005	2056	125	321	18	147	3
18	0.03	8.76	0.1245	0.0098	0.3594	0.0243	0.0226	0.0006	2022	145	312	18	144	4
19	0.71	32.12	0.1666	0.0120	0.5557	0.0467	0.0245	0.0005	2524	121	449	31	156	3
20	0.57	10.57	0.2652	0.0137	0.9947	0.0438	0.0298	0.0006	3277	81	701	22	189	4
21	0.63	17.98	0.3815	0.0176	1.8904	0.0915	0.0375	0.0009	3838	70	1078	32	237	6
22	0.55	42.38	0.0574	0.0031	0.1523	0.0075	0.0205	0.0003	506	119	144	7	131	2
23	0.23	24.54	0.1075	0.0063	0.2969	0.0163	0.0215	0.0004	1758	103	264	13	137	2
24	0.12	33.56	0.0955	0.0056	0.2599	0.0141	0.0210	0.0004	1537	111	235	11	134	2
25	0.08	10.95	0.3525	0.0190	1.5364	0.0819	0.0336	0.0009	3718	82	945	33	213	6
26	0.44	21.23	0.3571	0.0150	1.5462	0.0592	0.0334	0.0005	3738	69	949	24	212	3
27	0.37	1.83	0.7281	0.0319	17.3629	0.7181	0.1854	0.0048	-	-	2955	40	1096	26
28	0.04	7.97	0.1215	0.0082	0.3390	0.0206	0.0213	0.0004	1977	120	296	16	136	3
29	0.32	21.50	0.2495	0.0128	0.8657	0.0432	0.0265	0.0005	3183	81	633	24	168	3
30	0.46	31.50	0.0839	0.0059	0.2171	0.0133	0.0202	0.0004	1300	137	200	11	129	3
<b>108-1-b6 (Makeng)</b>														
1	0.94	4.56	0.4336	0.0297	2.1821	0.1769	0.0375	0.0013	4031	102	1175	56	237	8
2	1.11	6.77	0.1252	0.0095	0.3786	0.0238	0.0237	0.0006	2032	135	326	18	151	4
3	0.42	2.93	0.4673	0.0319	2.7365	0.1940	0.0450	0.0016	4141	101	1338	53	284	10
4	0.79	2.96	0.6953	0.0417	10.2987	0.5488	0.1155	0.0036	-	-	2462	49	705	21
5	0.40	6.80	0.4961	0.0417	2.8404	0.2343	0.0443	0.0022	4230	125	1366	62	279	14
6	0.19	4.24	0.5021	0.0264	3.4804	0.1802	0.0532	0.0015	4247	78	1523	41	334	9
7	0.25	4.29	0.1102	0.0108	0.3458	0.0244	0.0230	0.0007	1802	180	302	18	147	4
8	0.17	4.50	0.1748	0.0144	0.5955	0.0424	0.0253	0.0007	2603	137	474	27	161	4
9	0.12	3.75	0.4045	0.0231	2.3733	0.1326	0.0447	0.0014	3926	85	1235	40	282	9
10	0.29	3.81	0.0950	0.0145	0.3441	0.0374	0.0209	0.0008	1529	290	300	28	133	5
11	0.17	5.67	0.1250	0.0120	0.4242	0.0356	0.0233	0.0006	2028	172	359	25	148	4
12	0.35	4.24	0.5456	0.0246	6.8869	0.4221	0.0907	0.0039	4369	66	2097	54	559	23

(Continued on following page)

TABLE 3 (Continued) LA-ICPMS garnet U-Pb data for skarn rocks from the Makeng-style iron polymetallic deposits.

Spot	U	Th	207Pb/ 206 Pb		207 Pb/235U		206 Pb/238U		207Pb/206 Pb		207 Pb/235U		206 Pb/238U	
			ppm	ppm	Ratio	1σ	Ratio	1σ	Ratio	1σ	Age (Ma)	1σ	Age (Ma)	1σ
13	0.79	5.45	0.5889	0.0252	8.2782	0.4150	0.1048	0.0041	4481	62	2262	45	642	24
14	2.72	15.09	0.4251	0.0208	2.8987	0.1531	0.0500	0.0014	4400	73	1382	40	314	9
15	2.99	15.07	0.4617	0.0220	3.4461	0.1575	0.0549	0.0014	4123	71	1515	36	345	9
16	0.45	4.62	0.2967	0.0221	1.2369	0.0816	0.0316	0.0011	3453	116	817	37	201	7
17	0.25	5.12	0.3193	0.0244	1.5665	0.1422	0.0350	0.0015	3566	118	957	56	222	9
18	0.66	2.42	0.4373	0.0230	2.6376	0.1306	0.0460	0.0015	4043	79	1311	36	290	10
19	0.71	2.60	0.2372	0.0188	0.8748	0.0616	0.0286	0.0009	3102	132	638	33	182	5
20	0.15	4.14	0.3921	0.0289	2.1059	0.1352	0.0398	0.0013	3879	111	1151	44	252	8
21	0.50	4.72	0.1692	0.0144	0.6018	0.0509	0.0258	0.0008	2550	144	478	32	164	5
22	1.21	5.42	0.1847	0.0173	0.6328	0.0565	0.0240	0.0010	2696	155	498	35	153	6
23	0.21	3.80	0.1364	0.0143	0.4624	0.0386	0.0219	0.0007	2183	183	386	27	140	4
24	0.18	2.32	0.4007	0.0318	1.7772	0.1458	0.0335	0.0015	3912	121	1037	53	212	9
25	0.10	3.32	0.2240	0.0176	0.8708	0.0625	0.0284	0.0009	3010	127	636	34	180	6
26	0.68	3.37	0.5753	0.0323	6.3957	0.3214	0.0845	0.0025	4447	82	2032	44	523	15
27	0.59	3.79	0.4616	0.0286	2.2948	0.1296	0.0389	0.0015	4123	92	1211	40	246	9
<b>ZK7525-b1 (Makeng)</b>														
1	0.23	2.77	0.6239	0.0328	17.5861	0.8487	0.2029	0.0060	4565	76	2967	46	1191	32
2	0.06	2.09	0.3683	0.0347	1.9964	0.1627	0.0428	0.0017	3785	143	1114	55	270	11
3	0.00	1.31	0.5501	0.0575	4.0186	0.3264	0.0587	0.0029	4383	153	1638	66	368	18
4	0.06	1.54	0.5186	0.0303	5.8729	0.3032	0.0828	0.0024	4295	86	1957	45	513	14
5	0.00	3.33	0.6577	0.0340	36.8511	1.7438	0.3926	0.0076	4643	78	3690	47	2135	35
6	0.02	1.82	0.4471	0.0358	3.8427	0.2798	0.0632	0.0024	4076	119	1602	59	395	15
7	0.08	1.84	0.6491	0.0416	29.0486	1.6758	0.3169	0.0112	4622	94	3455	57	1774	55
8	0.03	2.22	0.6366	0.0339	13.8873	0.6181	0.1561	0.0038	4594	77	2742	42	935	21
9	0.10	2.03	0.6200	0.0391	10.9974	0.6007	0.1269	0.0041	4567	92	2523	51	770	24
10	0.09	1.85	0.4462	0.0360	2.6494	0.2005	0.0429	0.0019	4073	120	1314	56	271	12
11	0.04	1.34	0.5422	0.0357	7.1853	0.4034	0.0956	0.0036	4360	97	2135	50	589	21
12	0.31	5.83	0.6663	0.0352	29.7964	1.5244	0.3153	0.0091	4660	78	3480	50	1767	45
13	0.27	4.94	0.5370	0.0295	6.8047	0.4195	0.0898	0.0036	4346	80	2086	55	555	21
14	0.14	5.62	0.5825	0.0296	6.7949	0.3102	0.0845	0.0024	4465	75	2085	40	523	14
15	0.30	9.71	0.5703	0.0391	5.7821	0.3444	0.0761	0.0026	4434	100	1944	52	473	15
16	0.19	4.40	0.4055	0.0491	1.9113	0.1999	0.0378	0.0026	3931	183	1085	70	239	16
17	0.20	8.09	0.4268	0.0334	2.4378	0.1582	0.0433	0.0015	4006	117	1254	47	273	10
18	0.29	10.25	0.5885	0.0378	7.7209	0.4383	0.0949	0.0037	4480	94	2199	51	585	22
19	0.22	7.09	0.6551	0.0265	20.6765	0.7495	0.2237	0.0044	4636	58	3124	35	1301	23
20	0.14	4.67	0.2077	0.0208	0.8576	0.0769	0.0306	0.0013	2888	163	629	42	195	8
21	0.15	4.54	0.6044	0.0312	10.9048	0.5029	0.1306	0.0035	4520	75	2515	43	791	20
22	0.17	4.95	0.5425	0.0314	6.1762	0.3004	0.0835	0.0024	4361	85	2001	43	517	14
23	0.21	4.72	0.6086	0.0332	16.7701	0.7951	0.1999	0.0069	4529	79	2922	45	1175	37
24	0.19	6.78	0.5474	0.0293	6.7716	0.3131	0.0891	0.0026	4376	78	2082	41	550	15
25	0.22	7.63	0.6137	0.0292	13.8224	0.5782	0.1594	0.0039	4543	69	2738	40	954	22
26	0.06	3.33	0.6611	0.0329	26.2616	1.1962	0.2795	0.0070	4650	75	3356	45	1589	35
27	0.07	1.70	0.7000	0.0446	22.2869	1.2207	0.2310	0.0080	-	-	3196	53	1340	42
28	0.26	6.84	0.6050	0.0359	13.4717	0.6859	0.1576	0.0038	4520	86	2713	48	943	21

(Continued on following page)

TABLE 3 (Continued) LA-ICPMS garnet U-Pb data for skarn rocks from the Makeng-style iron polymetallic deposits.

Spot	U	Th	207Pb/ 206 Pb		207 Pb/235U		206 Pb/238U		207Pb/206 Pb		207 Pb/235U		206 Pb/238U	
			ppm	ppm	Ratio	1σ	Ratio	1σ	Ratio	1σ	Age (Ma)	1σ	Age (Ma)	1σ
<b>214-b9 (Makeng)</b>														
1	0.22	1.66	0.6476	0.0337	18.2123	0.8815	0.2034	0.0057	4620	75	3001	47	1194	31
2	1.89	0.43	0.3521	0.0330	2.0037	0.1797	0.0433	0.0017	3716	144	1117	61	273	11
3	0.29	0.35	0.5683	0.0504	4.4714	0.3107	0.0631	0.0027	4429	130	1726	58	394	16
4	4.33	0.85	0.6873	0.0376	39.2219	1.9702	0.4026	0.0080	4705	81	3751	50	2181	37
5	4.32	1.65	0.4728	0.0393	4.0125	0.2934	0.0640	0.0024	4159	124	1637	59	400	15
6	1.92	0.52	0.6628	0.0440	29.2187	1.7465	0.3153	0.0112	4652	99	3461	59	1767	55
7	2.94	1.06	0.6510	0.0359	13.9961	0.6509	0.1554	0.0038	4626	80	2749	44	931	21
8	0.71	0.72	0.7131	0.0420	32.7050	2.2300	0.3199	0.0136	-	-	3572	67	1789	66
9	1.70	1.05	0.6363	0.0402	11.1457	0.6205	0.1265	0.0042	4593	92	2535	52	768	24
10	2.10	0.72	0.4605	0.0397	2.5832	0.2177	0.0407	0.0020	4119	128	1296	62	257	12
11	1.50	0.62	0.5559	0.0366	7.3142	0.4170	0.0956	0.0036	4397	97	2151	51	589	21
12	0.23	0.51	0.6819	0.0362	30.3447	1.5802	0.3158	0.0092	4693	78	3498	51	1769	45
13	4.56	1.92	0.5485	0.0304	6.9331	0.4333	0.0901	0.0036	4377	81	2103	55	556	21
14	3.01	1.50	0.5940	0.0307	6.9263	0.3259	0.0849	0.0024	4494	76	2102	42	525	14
15	1.25	0.59	0.5805	0.0404	5.8967	0.3595	0.0766	0.0026	4460	101	1961	53	476	15
16	1.12	1.38	0.4120	0.0502	1.9501	0.2060	0.0381	0.0026	3954	184	1098	71	241	16
17	2.46	1.47	0.4394	0.0326	2.7387	0.1965	0.0464	0.0017	4050	111	1339	53	292	11
18	1.22	1.26	0.5842	0.0383	7.7194	0.4510	0.0960	0.0037	4469	96	2199	53	591	22
19	0.47	1.07	0.6508	0.0280	20.9695	0.8545	0.2308	0.0057	4626	62	3137	40	1339	30
20	0.80	1.15	0.5746	0.0318	10.2931	0.5042	0.1309	0.0038	4445	81	2461	45	793	22
21	2.19	1.18	0.5316	0.0327	5.8249	0.3025	0.0811	0.0025	4331	91	1950	45	503	15
22	1.42	1.24	0.5243	0.0286	6.5007	0.3129	0.0900	0.0026	4311	80	2046	42	556	15
23	0.61	1.09	0.5913	0.0284	12.9369	0.5678	0.1565	0.0042	4487	70	2675	41	937	23
24	0.55	1.22	0.6290	0.0326	24.6211	1.2098	0.2779	0.0076	4576	75	3293	48	1581	38
25	1.90	1.90	0.6604	0.0410	21.7912	1.1920	0.2405	0.0081	4647	93	3174	53	1389	42
26	0.66	1.99	0.7624	0.0374	64.0261	3.2036	0.5995	0.0225	-	-	4239	50	3028	90
27	0.78	1.43	0.7677	0.0358	54.5306	2.2318	0.5057	0.0144	-	-	4079	41	2638	62
28	0.50	1.80	0.6190	0.0323	10.0960	0.4652	0.1186	0.0037	4553	76	2444	43	723	21
29	1.22	1.75	0.3069	0.0293	1.2068	0.0803	0.0318	0.0012	3505	148	804	37	201	8
30	0.47	1.80	0.6552	0.0334	13.8713	0.6265	0.1508	0.0041	4636	74	2741	43	906	23
31	1.24	1.62	0.6521	0.0363	17.0459	0.8827	0.1855	0.0053	4629	80	2937	50	1097	29
32	0.35	1.26	0.6981	0.0337	26.6159	1.3560	0.2712	0.0088	-	-	3369	50	1547	45
33	0.77	1.62	0.4686	0.0343	3.8031	0.2486	0.0607	0.0020	4145	109	1593	53	380	12
34	0.22	1.58	0.4679	0.0408	2.9109	0.2173	0.0492	0.0021	4144	162	1385	56	310	13
35	0.53	1.57	0.6166	0.0413	9.5925	0.5477	0.1162	0.0038	4548	97	2396	53	708	22
36	0.24	1.31	0.5042	0.0367	3.4483	0.2213	0.0528	0.0019	4253	107	1515	51	331	12
37	0.22	1.16	0.6342	0.0335	8.2359	0.3839	0.0947	0.0025	4589	77	2257	42	584	14
38	0.16	1.02	0.5573	0.0367	5.4621	0.3017	0.0724	0.0024	4400	97	1895	47	450	14
39	1.06	1.35	0.6693	0.0352	12.7570	0.5790	0.1383	0.0038	4666	78	2662	43	835	22
40	0.34	1.43	0.5314	0.0328	4.1324	0.2090	0.0568	0.0017	4331	90	1661	41	356	10
41	0.20	1.25	0.6691	0.0358	12.5708	0.5670	0.1357	0.0036	4666	79	2648	42	820	20
42	0.34	1.95	0.4735	0.0276	4.1350	0.2066	0.0650	0.0023	4161	86	1661	41	406	14
43	0.27	1.43	0.7715	0.0346	44.8081	1.8817	0.4117	0.0092	-	-	3883	42	2223	42
44	0.18	1.14	0.7576	0.0467	35.2102	1.9867	0.3374	0.0108	-	-	3645	56	1874	52

(Continued on following page)

TABLE 3 (Continued) LA-ICPMS garnet U-Pb data for skarn rocks from the Makeng-style iron polymetallic deposits.

Spot	U	Th	207Pb/ 206 Pb		207 Pb/235U		206 Pb/238U		207Pb/206 Pb		207 Pb/235U		206 Pb/238U	
			ppm	ppm	Ratio	1σ	Ratio	1σ	Ratio	1σ	Age (Ma)	1σ	Age (Ma)	1σ
45	0.26	1.86	0.3002	0.0302	1.4530	0.1686	0.0334	0.0017	3471	157	911	70	212	10
46	0.27	1.80	0.4826	0.0435	2.6538	0.1808	0.0442	0.0017	4191	133	1316	50	279	10
47	0.20	1.59	0.3486	0.0343	1.5584	0.1219	0.0360	0.0013	3701	151	954	48	228	8
48	0.15	1.56	0.5385	0.0373	5.4403	0.3266	0.0749	0.0025	4350	102	1891	52	466	15
<b>ZK405-b13(Luoyang)</b>														
1	0.27	5.85	0.0597	0.0079	0.1834	0.0242	0.0229	0.0007	594	289	171	21	146	4
2	0.28	4.71	0.3951	0.0210	2.3081	0.1146	0.0426	0.0010	3891	80	1215	35	269	6
3	0.32	5.55	0.4057	0.0257	2.1981	0.1236	0.0401	0.0011	3931	101	1180	39	254	7
4	0.36	5.10	0.5241	0.0337	3.7563	0.2152	0.0525	0.0017	4310	95	1583	46	330	11
5	0.38	6.29	0.0777	0.0140	0.2065	0.0312	0.0213	0.0008	1139	366	191	26	136	5
6	0.37	5.38	0.0924	0.0113	0.2626	0.0282	0.0219	0.0007	1476	233	237	23	140	4
7	0.33	5.26	0.0885	0.0106	0.2587	0.0252	0.0230	0.0008	1392	232	234	20	147	5
8	0.40	6.92	0.2255	0.0207	0.9103	0.0852	0.0284	0.0010	3020	148	657	45	180	6
9	0.24	3.57	0.6084	0.0361	6.1001	0.4115	0.0694	0.0028	4528	86	1990	59	433	17
10	0.19	5.54	0.0688	0.0109	0.1922	0.0241	0.0220	0.0007	894	330	179	21	140	4
11	0.18	3.60	0.7043	0.0407	19.5640	1.2119	0.1928	0.0081	-	-	3070	60	1137	44
12	0.79	3.57	0.5231	0.0312	4.9819	0.2636	0.0681	0.0019	4308	88	1816	45	424	11
13	0.83	3.15	0.7001	0.0316	28.2689	1.3376	0.2828	0.0080	-	-	3428	46	1606	40
14	0.57	2.92	0.7568	0.0350	97.5009	4.3223	0.8959	0.0161	-	-	4661	45	4124	55
15	0.89	3.49	0.7136	0.0332	78.6587	3.6026	0.7780	0.0267	-	-	4445	46	3710	97
16	0.46	7.95	0.5335	0.0261	4.5184	0.2469	0.0593	0.0018	4337	72	1734	45	371	11
17	0.78	3.63	0.7479	0.0391	74.2827	4.0644	0.7019	0.0219	-	-	4388	55	3428	83
<b>BL23(Luoyang)</b>														
1	0.62	12.40	0.5453	0.0279	5.5355	0.2573	0.0710	0.0014	4369	75	1906	40	442	8
2	0.36	13.14	0.5162	0.0239	4.9035	0.2246	0.0665	0.0018	4288	68	1803	39	415	11
3	0.43	9.52	0.3367	0.0198	2.1276	0.1435	0.0434	0.0015	3648	90	1158	47	274	9
4	0.82	13.56	0.3391	0.0170	2.0941	0.1268	0.0420	0.0014	3659	77	1147	42	266	9
5	0.65	13.34	0.3097	0.0171	1.4384	0.0778	0.0327	0.0011	3519	85	905	32	207	7
6	0.18	70.20	0.0684	0.0039	0.2090	0.0103	0.0215	0.0004	880	114	193	9	137	2
7	1.09	12.71	0.3223	0.0149	1.9169	0.0790	0.0416	0.0008	3581	71	1087	27	263	5
8	0.51	10.92	0.1433	0.0093	0.5080	0.0309	0.0252	0.0006	2333	113	417	21	160	4
9	0.60	12.23	0.0695	0.0051	0.2222	0.0148	0.0228	0.0005	922	152	204	12	145	3
10	0.26	43.49	0.1403	0.0073	0.5099	0.0251	0.0254	0.0005	2231	90	418	17	162	3
11	0.53	16.92	0.4639	0.0237	4.3702	0.1961	0.0661	0.0015	4131	76	1707	37	413	9
12	0.35	8.61	0.5186	0.0272	6.4925	0.3460	0.0877	0.0028	4295	77	2045	47	542	17
13	0.37	9.72	0.5837	0.0308	11.6576	0.5219	0.1405	0.0036	4468	77	2577	42	848	20
14	0.63	11.74	0.4061	0.0210	2.9096	0.1380	0.0503	0.0015	3932	78	1384	36	317	9
15	0.56	10.85	0.5065	0.0216	6.5565	0.2977	0.0907	0.0029	4260	63	2054	40	559	17
16	0.45	11.35	0.5081	0.0223	6.5896	0.3300	0.0900	0.0031	4265	65	2058	44	556	18
17	0.66	12.82	0.5194	0.0244	6.1065	0.2766	0.0819	0.0021	4297	69	1991	40	507	13
18	0.61	114.40	0.2560	0.0125	1.1599	0.0554	0.0314	0.0009	3222	77	782	26	199	6
19	0.29	8.85	0.5275	0.0227	8.0546	0.3646	0.1057	0.0031	4320	64	2237	41	648	18
20	0.68	12.93	0.4070	0.0259	2.7360	0.1714	0.0471	0.0016	3936	96	1338	47	297	10

(Continued on following page)

TABLE 3 (Continued) LA-ICPMS garnet U-Pb data for skarn rocks from the Makeng-style iron polymetallic deposits.

Spot	U	Th	207Pb/ 206 Pb		207 Pb/235U		206 Pb/238U		207Pb/206 Pb		207 Pb/235U		206 Pb/238U	
			ppm	ppm	Ratio	1σ	Ratio	1σ	Ratio	1σ	Age (Ma)	1σ	Age (Ma)	1σ
21	0.19	12.80	0.0739	0.0056	0.2358	0.0162	0.0224	0.0005	1040	153	215	13	143	3
22	0.71	11.29	0.3722	0.0201	2.6009	0.1608	0.0478	0.0014	3800	82	1301	45	301	9
23	0.53	22.85	0.1327	0.0088	0.4906	0.0338	0.0256	0.0006	2200	121	405	23	163	4
24	0.60	58.06	0.0436	0.0038	0.1320	0.0108	0.0213	0.0004	-	-	126	10	136	3
25	0.61	33.12	0.1540	0.0097	0.5692	0.0327	0.0259	0.0005	2391	108	458	21	165	3
26	0.51	10.44	0.3427	0.0223	1.8143	0.1191	0.0368	0.0013	3675	100	1051	43	233	8
27	0.36	24.23	0.1519	0.0094	0.5756	0.0316	0.0261	0.0005	2369	106	462	20	166	3
28	0.36	11.67	0.3005	0.0177	1.8585	0.0963	0.0424	0.0010	3473	91	1066	34	268	6
<b>ZK403-b92 (Dapai)</b>														
1	6.38	15.29	0.1025	0.0090	0.3113	0.0283	0.0211	0.0005	1669	167	275	22	134	3
2	4.38	22.12	0.2908	0.0238	1.6083	0.1707	0.0357	0.0029	3422	128	973	66	226	18
3	5.83	13.23	0.3110	0.0175	1.3736	0.0770	0.0314	0.0007	3526	87	878	33	199	5
4	3.85	20.12	0.1367	0.0120	0.4726	0.0493	0.0232	0.0006	2187	153	393	34	148	4
5	3.18	17.71	0.0904	0.0070	0.2731	0.0206	0.0216	0.0005	1435	148	245	16	138	3
6	3.96	20.51	0.1044	0.0061	0.3192	0.0180	0.0219	0.0004	1706	109	281	14	140	2
7	4.33	16.34	0.0904	0.0070	0.2669	0.0190	0.0216	0.0005	1433	147	240	15	138	3
8	4.12	16.38	0.0736	0.0067	0.2227	0.0189	0.0218	0.0005	1031	185	204	16	139	3
9	3.66	16.24	0.0563	0.0045	0.1634	0.0121	0.0210	0.0004	465	180	154	11	134	3
10	4.98	17.54	0.1258	0.0081	0.4272	0.0263	0.0243	0.0005	2040	113	361	19	155	3
11	3.00	14.73	0.0689	0.0058	0.2020	0.0159	0.0213	0.0005	894	174	187	13	136	3
12	3.22	14.76	0.1645	0.0139	0.5798	0.0443	0.0256	0.0007	2502	143	464	28	163	4
13	6.33	12.27	0.1612	0.0132	0.5127	0.0370	0.0234	0.0006	2469	144	420	25	149	4
14	6.36	13.84	0.1458	0.0156	0.5955	0.0812	0.0249	0.0009	2298	185	474	52	159	5
15	0.35	3.64	0.5805	0.0296	7.0387	0.4870	0.0854	0.0043	4460	74	2116	62	528	26
16	4.34	13.70	0.4408	0.0233	3.1375	0.1442	0.0506	0.0011	4055	79	1442	35	318	6
17	2.49	14.81	0.1592	0.0113	0.5709	0.0442	0.0251	0.0007	2448	121	459	29	160	4
18	3.21	16.66	0.3608	0.0210	1.8279	0.1355	0.0355	0.0016	3753	89	1056	49	225	10
19	4.31	13.58	0.2332	0.0147	0.8684	0.0488	0.0267	0.0007	3076	101	635	27	170	4
20	3.30	16.25	0.1363	0.0117	0.4428	0.0399	0.0225	0.0007	2181	145	372	28	143	4
21	5.50	17.38	0.3170	0.0171	1.5066	0.0928	0.0327	0.0008	3567	83	933	38	208	5
22	9.64	17.23	0.1372	0.0098	0.4618	0.0297	0.0242	0.0007	2192	124	386	21	154	4
23	6.88	14.74	0.3104	0.0189	1.4818	0.0998	0.0336	0.0013	3523	94	923	41	213	8
24	6.39	18.95	0.1673	0.0140	0.6146	0.0555	0.0253	0.0007	2531	141	486	35	161	4
25	3.35	15.73	0.0844	0.0069	0.2761	0.0236	0.0229	0.0005	1303	155	248	19	146	3
<b>ZK403-b67 (Dapai)</b>														
1	1.45	16.94	0.2843	0.0185	1.2824	0.0794	0.0314	0.0008	3387	102	838	35	200	5
2	0.64	10.19	0.5129	0.0301	4.4107	0.3155	0.0578	0.0024	4279	87	1714	59	362	14
3	1.11	22.78	0.0637	0.0049	0.1889	0.0130	0.0216	0.0005	733	163	176	11	138	3
4	0.55	20.79	0.4067	0.0256	2.2012	0.1290	0.0382	0.0014	3934	95	1181	41	242	8
5	0.58	22.85	0.1937	0.0152	0.7254	0.0643	0.0255	0.0007	2774	129	554	38	163	5
6	0.22	9.46	0.0887	0.0096	0.2856	0.0304	0.0226	0.0007	1398	208	255	24	144	4
7	0.69	5.56	0.2481	0.0228	0.9697	0.0753	0.0297	0.0011	3173	145	688	39	189	7
8	0.87	5.69	0.4668	0.0261	3.2118	0.1680	0.0498	0.0015	4140	83	1460	41	313	9

(Continued on following page)

TABLE 3 (Continued) LA-ICPMS garnet U-Pb data for skarn rocks from the Makeng-style iron polymetallic deposits.

Spot	U	Th	207Pb/ 206 Pb		207 Pb/235U		206 Pb/238U		207Pb/206 Pb		207 Pb/235U		206 Pb/238U	
			ppm	ppm	Ratio	1σ	Ratio	1σ	Ratio	1σ	Age (Ma)	1σ	Age (Ma)	1σ
9	0.28	17.44	0.0703	0.0048	0.2084	0.0147	0.0209	0.0004	937	141	192	12	133	3
10	0.69	35.38	0.0585	0.0050	0.1685	0.0133	0.0207	0.0004	546	189	158	12	132	2
11	0.19	21.81	0.0491	0.0039	0.1449	0.0110	0.0211	0.0004	154	178	137	10	135	3
12	0.43	2.01	0.4007	0.0565	1.6943	0.1957	0.0344	0.0020	3912	214	1006	74	218	12
13	0.39	9.19	0.5353	0.0268	5.8320	0.3417	0.0762	0.0027	4342	73	1951	51	473	16
14	0.17	5.53	0.3864	0.0321	2.7138	0.2367	0.0486	0.0018	3857	126	1332	65	306	11
15	0.72	13.30	0.4201	0.0208	2.5875	0.1232	0.0434	0.0012	3982	74	1297	35	274	7
16	0.55	14.94	0.2787	0.0244	1.9319	0.2393	0.0379	0.0021	3367	137	1092	83	240	13
17	0.43	8.10	0.2569	0.0170	1.1437	0.0704	0.0313	0.0008	3228	104	774	33	199	5
18	0.47	17.02	0.2646	0.0210	1.1339	0.0882	0.0304	0.0012	3276	125	770	42	193	7
19	0.17	3.39	0.1314	0.0153	0.4535	0.0571	0.0243	0.0010	2117	206	380	40	155	7
20	0.37	22.48	0.1834	0.0134	0.6469	0.0406	0.0249	0.0007	2684	155	507	25	158	5
21	0.37	17.63	0.0713	0.0056	0.2133	0.0158	0.0217	0.0005	965	163	196	13	139	3
22	0.33	13.69	0.3515	0.0184	1.8779	0.1130	0.0370	0.0011	3714	80	1073	40	234	7
23	0.68	13.20	0.1138	0.0116	0.3765	0.0426	0.0228	0.0006	1861	185	324	31	145	4
24	0.27	10.99	0.1947	0.0179	0.7718	0.0763	0.0278	0.0011	2782	151	581	44	177	7
25	0.42	16.94	0.0663	0.0055	0.1826	0.0138	0.0207	0.0006	817	176	170	12	132	4
26	0.88	16.28	0.3239	0.0171	1.4577	0.0857	0.0317	0.0008	3589	81	913	35	201	5
27	1.28	33.45	0.0634	0.0047	0.1864	0.0133	0.0214	0.0005	720	159	174	11	136	3
28	1.81	8.02	0.0664	0.0073	0.1875	0.0196	0.0206	0.0007	820	231	175	17	131	4
29	1.84	8.65	0.0721	0.0089	0.2076	0.0229	0.0209	0.0007	989	256	192	19	133	4
30	1.23	11.29	0.2108	0.0165	0.8196	0.0653	0.0276	0.0008	2922	128	608	36	175	5
<b>PTPD-b21 (Dapai)</b>														
1	1.45	20.38	0.0946	0.0077	0.2604	0.0214	0.0205	0.0006	1520	149	235	17	131	4
2	1.20	21.97	0.2246	0.0211	0.5433	0.0488	0.0220	0.0010	3014	151	441	32	140	7
3	1.54	28.78	0.2360	0.0260	0.5458	0.0537	0.0210	0.0010	3094	177	442	35	134	6
4	1.52	27.94	0.3648	0.0895	0.5987	0.0503	0.0209	0.0010	3770	381	476	32	133	6
5	1.46	25.93	0.3178	0.0412	0.6831	0.0746	0.0211	0.0011	3561	201	529	45	134	7
6	1.26	21.45	0.1008	0.0081	0.2664	0.0208	0.0202	0.0005	1639	151	240	17	129	3
7	1.60	29.86	0.1231	0.0127	0.3149	0.0226	0.0221	0.0007	2002	185	278	17	141	5
8	2.36	28.23	0.1597	0.0158	0.3664	0.0258	0.0202	0.0007	2454	169	317	19	129	5
9	1.18	21.38	0.1171	0.0119	0.2825	0.0264	0.0207	0.0007	1913	182	253	21	132	4
10	0.02	14.47	0.1363	0.0139	0.3462	0.0281	0.0212	0.0008	2181	179	302	21	135	5
11	0.64	21.70	0.1981	0.0245	0.4882	0.0398	0.0211	0.0009	2810	204	404	27	135	6
12	0.13	11.98	0.2372	0.0310	0.5176	0.0386	0.0221	0.0012	3102	210	424	26	141	8
13	0.18	6.54	0.1037	0.0088	0.2532	0.0190	0.0211	0.0007	1691	157	229	15	134	4
14	0.31	9.91	0.0862	0.0063	0.2416	0.0201	0.0206	0.0006	1343	141	220	16	131	4
15	1.11	15.56	0.0699	0.0070	0.1855	0.0164	0.0208	0.0006	928	207	173	14	133	4
16	1.28	20.38	0.3167	0.0794	0.5793	0.0534	0.0212	0.0011	3554	397	464	34	135	7
17	1.01	17.78	0.1285	0.0115	0.3421	0.0255	0.0214	0.0007	2077	159	299	19	136	4
18	0.31	7.68	0.0598	0.0050	0.1697	0.0137	0.0213	0.0004	594	151	159	12	136	2
19	0.39	13.03	0.0842	0.0089	0.2433	0.0223	0.0225	0.0006	1298	208	221	18	144	4
20	0.31	35.86	0.0738	0.0053	0.2046	0.0148	0.0205	0.0005	1035	145	189	13	131	3
21	0.30	29.39	0.1051	0.0097	0.2875	0.0253	0.0221	0.0006	1717	170	257	20	141	4
22	1.23	21.29	0.2345	0.0258	0.6071	0.0621	0.0225	0.0010	3083	178	482	39	144	6

(Continued on following page)

TABLE 3 (Continued) LA-ICPMS garnet U-Pb data for skarn rocks from the Makeng-style iron polymetallic deposits.

Spot	U ppm	Th ppm	207Pb/ 206 Pb		207 Pb/235U		206 Pb/238U		207Pb/206 Pb		207 Pb/235U		206 Pb/238U	
			Ratio	1σ	Ratio	1σ	Ratio	1σ	Age (Ma)	1σ	Age (Ma)	1σ	Age (Ma)	1σ
23	0.41	13.30	0.1225	0.0096	0.3084	0.0246	0.0191	0.0006	1994	140	273	19	122	4
24	0.23	56.34	0.1617	0.0178	0.3962	0.0350	0.0206	0.0007	2473	186	339	25	132	4
25	0.39	9.54	0.1014	0.0099	0.2743	0.0249	0.0204	0.0006	1650	182	246	20	130	4
26	0.40	10.63	0.0882	0.0072	0.2467	0.0192	0.0211	0.0005	1387	162	224	16	135	3

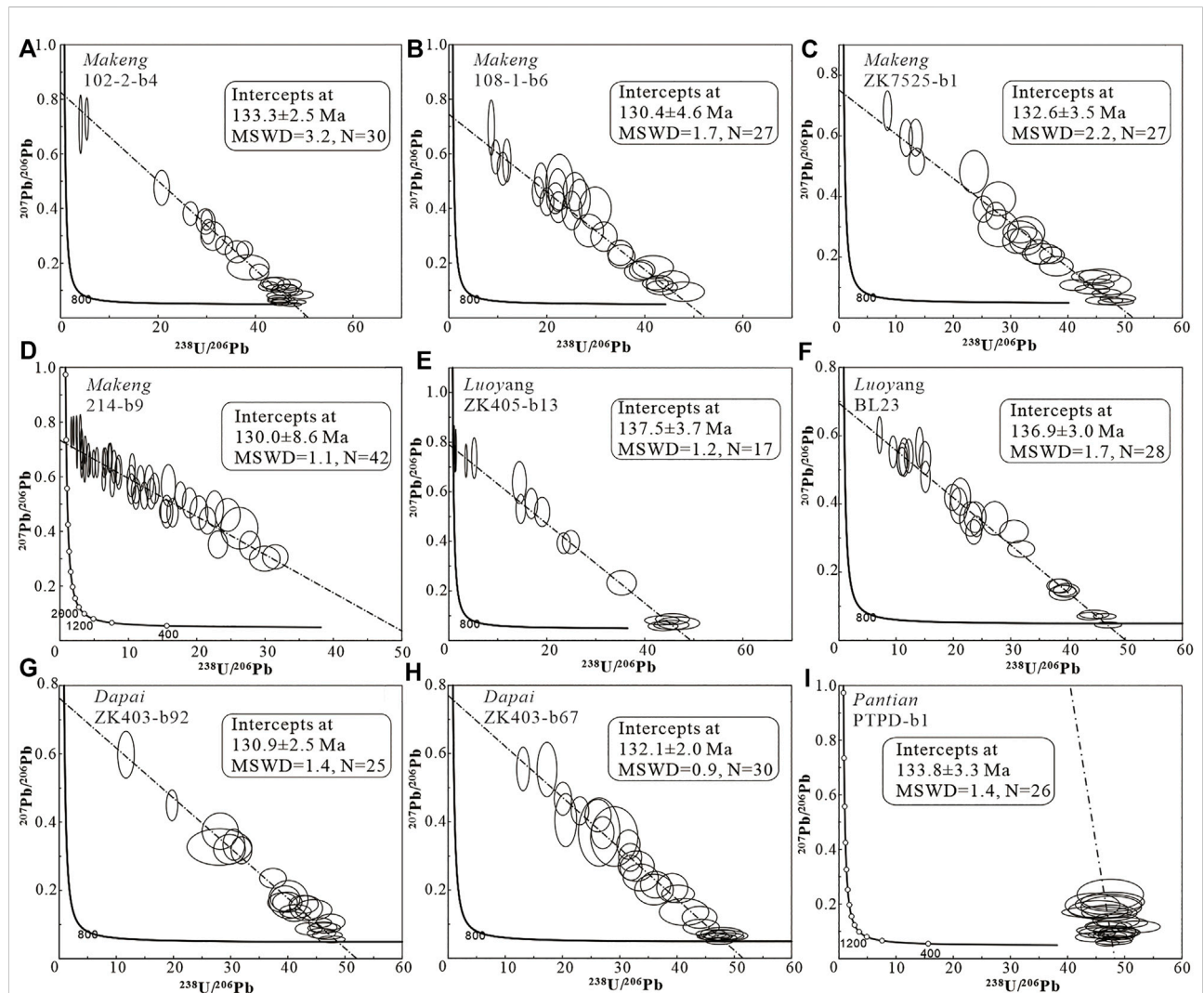


FIGURE 5

Tera-Wasserburg lower interception ages of Garnet from Makeng-style iron deposits. MSWD, mean squared weighted deviation; N, number of the spots.

TABLE 4 Geochronological results of Makeng-style Fe-polymetallic deposits.

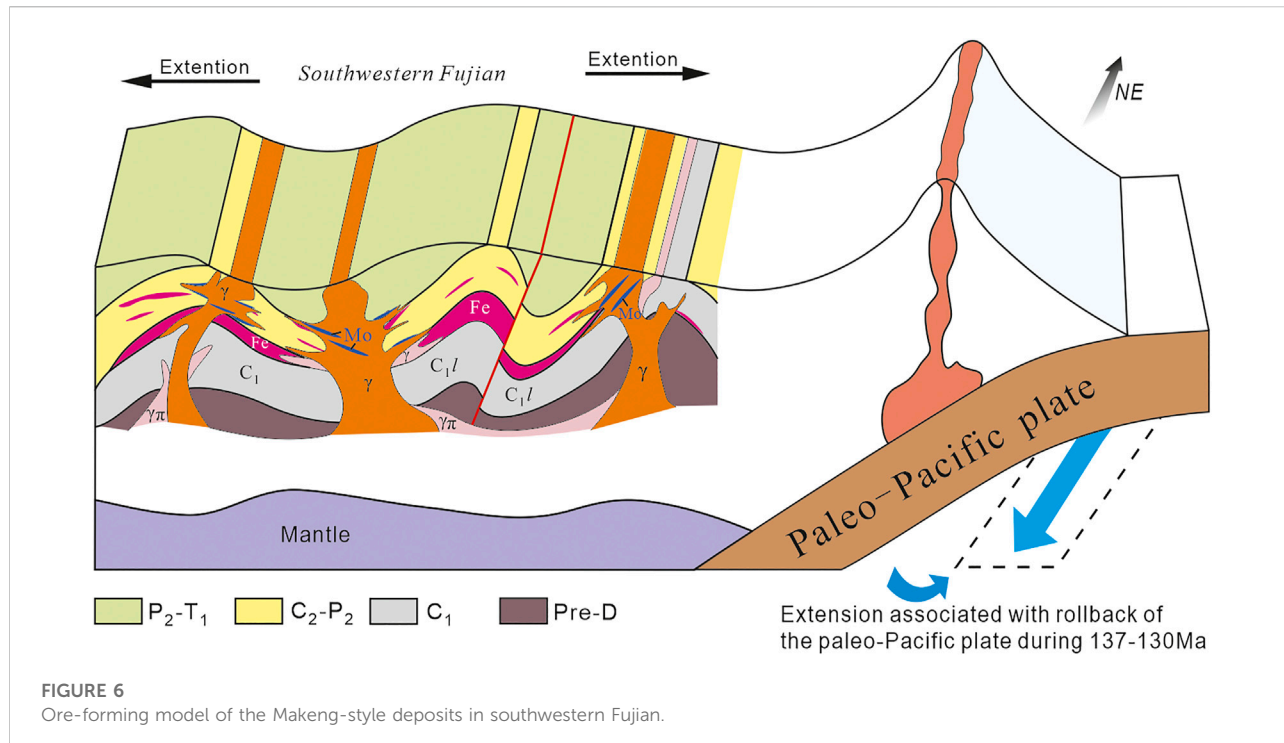
Testing objects	Age (Ma)	Sample no.	Methods	Data source
Makeng deposit	132.04 ± 0.61	D3083-b1	Zircon U-Pb	Wang et al. (2015)
	132.43 ± 0.84	D3086-b1		
	130 ± 1	JZ02		Zhang et al. (2013)
	129 ± 1	JZ03		
	136.0 ± 1.7	97LB4-1		
	154.9 ± 0.9	CM218-13		Yan (2013)
	152.7 ± 1.4	MK03		Wang et al. (2017a)
	161.2 ± 4.9	MK420	Garnet Sm-Nd	Wang et al. (2010)
	133.0 ± 0.8	MK24-MK77	Mobdenite Re-Os	Zhang et al. (2012a)
	133.2 ± 2.5	102-2-b4	Garnet U-Pb	This study
	130.4 ± 4.6	108-1-b6		
	132.6 ± 3.5	ZK7525-b1		
	130.0 ± 8.6	214-b9		
Dapai deposit	131.72 ± 0.41	ZK3102-b12	Zircon U-Pb	Yuan et al. (2014)
	132.35 ± 0.83	ZK403-b21		
	150.23±	DP08-07		Yuan et al. (2020)
	134.8 ± 1.2	ZK302	Mobdenite Re-Os	Yuan et al. (2014)
	130.9 ± 2.5	ZK403-b92	Garnet U-Pb	This study
	132.1 ± 2.0	ZK403-b67		
Luoyang deposit	131.31 ± 0.66	ZK1108-b1	Zircon U-Pb	Wang et al. (2021)
	137.2 ± 2.3	BL130		
	154.1 ± 1.4	ZK1108-b27		Yu. (2017)
	133.0 ± 1.9	BL128	Mobdenite Re-Os	Zhang et al. (2012b)
	137.5 ± 3.7	ZK405-b13	Garnet U-Pb	This study
	136.9 ± 3.0	BL23		
Pantian deposit	131.68 ± 0.48	ZK1204-b1	Zircon U-Pb	Lai et al. (2014)
	133.8 ± 3.3	PTPD-b1	Garnet U-Pb	This study

from the Pantian deposit yielded a lower interception age of  $133.8 \pm 3.3$  Ma, which was close to the zircon U-Pb age of  $131.7 \pm 0.5$  Ma (Lai et al., 2014).

Together with the zircon U-Pb and molybdenite Re-Os dating results mentioned above and our new garnet U-Pb analysis results, we can draw a conclusion that the mineralization age constrained by associated minerals of Makeng-style deposits mainly concentrated around 137 Ma to 130 Ma (Table 4). This research can well resolve the disagreement about the mineralization age of the Makeng-style deposits due to a lack of direct chronological evidence. It shows that the magnetite and molybdenite are nearly simultaneous and consistent with the emplacement age of the Cretaceous granites, which indicates that the magnetite mineralization may be related to the granites.

## Ore deposit type

The ore genesis of the Makeng-style Fe polymetallic deposits has been a controversial issue since they were discovered, and different genesis theories exist such as the marine sedimentation and hydrothermal modification, strata-bound skarn alteration, and silica-calcareous-plane mineralization hypotheses (Han and Ge, 1983; Wang et al., 2018a). A major reason for the controversy is the lack of direct chronological constraints. Magnetite ore bodies of the Makeng-style deposits mainly formed on the interface between Lower-Middle Permian carbonates and Late Devonian—Early Carboniferous clastic rocks, which caused the controversial understanding on the relationship between the mineralization and the granites. In addition, zircon U-Pb ages show that emplacement of the granites occurred in two main stages: ca. (160–150) Ma and ca. (135–130) Ma (Yan, 2013; Yu, 2017; Yuan et al., 2020); thus, it yields a



significant controversy on the genesis due to the lack of more direct evidences and the different interpretation of the mineralization age. In this paper, ore-bearing garnet samples collected from different orebodies and ore deposits were selected to provide new direct chronological constraints on ore genesis, and all the garnet U-Pb dating results for these four deposits were close overall, which indicated that the mineralization of Makeng-style deposits was related to Cretaceous granites (ca. 137–130 Ma).

The rare Earth element analysis results of representative ore-bearing garnet samples showed that the REE contents and chondrite-normalized REE patterns were distinct between different deposits. The total REE contents of garnet samples from the Makeng and Luoyang deposits were relatively low (22.29–68.26 ppm and 26.41–66.56 ppm) with features LREE (light rare Earth element) enrichment and HREE (heavy rare Earth element) depletion and positive Eu anomalies. The rare Earth element distribution features were similar to those of garnet formed by magmatic hydrothermal action, and the REE distribution types were similar to granites with REE decreases in garnet due to the dilutive effect of transudation (Auwera and Andre, 1991; Hong et al., 2012). In addition, the REE distribution features are similar to those of garnets from the Huanggangliang Sn-Fe deposit (Wang et al., 2002), Huangshaping W-M-Pb-Zn deposit (Ding et al., 2018a; Ding et al., 2018b) and Mengku Fe deposit (Yang et al., 2007), and they are regarded as typical skarn polymetallic deposits. The REE contents of garnet samples from the Dapai and Pantian deposits were relatively higher than those of the Makeng and Luoyang deposits, with total REE contents ( $\Sigma$ REE) of 216.49–526.53 ppm and 117.55–41–396.30 ppm, respectively. It showed flat features

of the REE distribution curves on the chondrite-normalized REE patterns with weak negative Eu anomalies, which were different from the Makeng and Luoyang deposit. The reason for this difference may be the distinct compositions of the mineralizing fluid. These mineralized bodies of Dapai and Pantian deposits locate in the contact zone of the granites and have similar hydrothermal components, and therefore it may be a major factor causing their relatively high REE contents and negative Eu anomalies. Unlike the Dapai and Pantian deposits, mineralized bodies of the Makeng and Luoyang deposits mainly locate on the interface between the Lower-Middle Permian carbonates and Late Devonian–Early Carboniferous clastic rocks. Therefore, it indicates that the ore-forming process may be distinct due to different mineralizing fluid for these deposits.

In summary, garnet U-Pb dating results of different deposits and different ore bodies of the same deposit showed that the ore-forming ages of the Makeng-style iron-polymetallic deposits were relatively close (concentrated among 137–130 Ma) with those of the zircon U-Pb ages of granites, indicating that the formation of magnetite was closely related to Cretaceous granite emplacement. The rare Earth element analysis results REE distribution features showed that these Makeng-style deposits are similar to typical skarn deposits with features of magmatic hydrothermal fluid, but there were some obvious differences between different deposits, indicating that there may be some differences in the mineralizing fluid and ore-forming process between different deposits.

## Metallogenic tectonic setting

A large-scale magmatic activity and mineralization event occurred in eastern China during the Yanshanian period; thus, studying the geochemical dynamic background and genesis mechanism of the deposit is of great significance to understand the Mesozoic tectonic transformation in eastern China and guide ore prospecting. Determining the mineralization age is a premise and key to understand the ore genesis and metallogenic mechanism, and therefore, the purpose of this study is to accurately determine the mineralization age and provide a reference for understanding the metallogenic mechanism and tectonic background of the iron-polymetallic deposits in the western margin of the Paleo-Pacific Plate.

Located on the southeastern margin of the Cathaysian Plate, the Makeng-style iron-polymetallic deposits are controversial due to their unique metallogenic geological characteristics, especially the controversy focused on the metallogenic age and metallogenic tectonic setting (Yan, 2013; Wang et al., 2018b; Zhang et al., 2018b). Our garnet U-Pb dating results provide more direct chronological evidence for the relationship between mineralization and Cretaceous granite bodies, and it proves that mineralization occurred at approximately 137–130 Ma rather than at 150 Ma or earlier time. Previous studies showed that the South China continent underwent a tectonic transition in the Early Cretaceous, that is, the transition from a compressional tectonic system dominated by intracontinental orogeny in the middle and late Jurassic to an extensional tectonic system in the early Cretaceous (Dong et al., 2008; Xing et al., 2008; Zhang et al., 2012c; Li et al., 2012). The possible deep dynamic mechanism for this tectonic transition is the rollback of the paleo-Pacific plate with a subduction dip angle of the subducting oceanic crust plate increasing from low-angle subduction to high-angle subduction, the retreat of the trench, and thickening of the crust, which caused the extensional collapse of the thickened continental crust under a relaxed stress environment (Zhang et al., 2012c; Li et al., 2012). In addition, the metallogenic tectonic background could be reflected by research on the diagenetic tectonic environment of the granites which are closely related to mineralization. The whole-rock geochemical results indicate that the granites from the Makeng, Luoyang, Dapai, and Pantian deposits are high-Si, high-K calc-alkaline and metaluminous to weakly peraluminous rocks, with features of highly fractionated I-type granites, which reflected an extensional tectonic setting with features of the transformational tectonic environment (Zhang et al., 2012b; Lai et al., 2014; Wang et al., 2015; Wang et al., 2021). Therefore, we believe that the Makeng-style iron-polymetallic deposits may have been

formed in an extensional tectonic environment caused by rollback after the subduction of the paleo-Pacific plate (Figure 6), with features of a transitional tectonic system.

## Conclusion

- 1) The garnet U-Pb dating method was applied to reveal the mineralization age and genesis of Makeng-style deposits, yielding 137–130 Ma ages for nine ore-bearing garnet samples from different deposits and orebodies of the same deposit.
- 2) The garnet U-Pb dating results (137–130 Ma) are consistent with the zircon U-Pb and molybdenite ages, which provides more direct evidence of the mineralization age for the Makeng-style deposits and indicates that the magnetite was closely related to Cretaceous granite emplacement.
- 3) Rare Earth element analysis results and REE patterns showed that there were typical skarn deposits, but obvious differences in the REE distribution types between different deposits, indicating that the ore-forming process may be distinct due to different mineralizing fluid for these deposits.
- 4) The Makeng-style iron-polymetallic deposits may have been formed in an extensional tectonic environment caused by rollback after subduction of the Paleo-Pacific Plate.

## Data availability statement

The original contributions presented in the study are included in the article/Supplementary Material, further inquiries can be directed to the corresponding author.

## Author contributions

SW: completion of manuscript KC: data treating DZ: writing guidance Others: Field and experimental assistance.

## Funding

This work was supported by the Fundamental Research Projects from the Institute of Geomechanics, Chinese Academy of Geological Sciences, National Natural Science Foundation of China (No. 41873063), and projects from the China Geological Survey (No. DD20221644 and 12120113089600).

## Acknowledgments

We are indebted to Yueheng Yang senior engineer from the Institute of Geology and Geophysics, Chinese Academy of Sciences,

for his kind assistance in providing standard samples. Great thanks to the reviewers and editors for their helpful comments.

## Conflict of interest

The authors declare that the research was conducted in the absence of any commercial or financial relationships that could be construed as a potential conflict of interest.

## References

- Auwera, J. V., and Andre, L. (1991). Trace elements (REE) and isotopes (O, C, Sr) to characterize the metasomatic fluid sources: Evidence from the skarn deposit (Fe, W, Cu) of traversella (ivrea, Italy). *Contr. Mineral. Pet.* 106, 325–339. doi:10.1007/bf00324561
- Chen, S. R., Xie, J. H., Xu, C. N., and Guo, W. W. (1985). The origin of makeng iron deposit, fujian. *Geochimica* 4, 350–357. doi:10.19700/j.0379-1726.1985.04.008
- Chen, W., Zhang, W. Q., Simonetti, A., and Jian, S. Y. (2016). Mineral chemistry of melanite from calcitic ijolite, the Oka carbonatite complex, Canada: Implications for multi-pulse magma mixing. *J. Earth Sci.* 27, 599–610. doi:10.1007/s12583-016-0715-3
- Deng, X. D., Li, J. W., Luo, T., and Wang, H. Q. (2017). Dating magmatic and hydrothermal processes using andradite-rich garnet U-Pb geochronometry. *Contrib. Mineral. Pet.* 172, 71–81. doi:10.1007/s00410-017-1389-2
- Ding, T., Ma, D. S., Lu, J. J., and Zhang, R. Q. (2018b). Magnetite as an indicator of mixed sources for W-Mo-Pb-Zn mineralization in the Huangshaping polymetallic deposit, southern Hunan Province, China. *Ore Geol. Rev.* 95, 65–78. doi:10.1016/j.oregeorev.2018.02.019
- Ding, T., Ma, D. S., Lu, J. J., and Zhang, R. Q. (2018a). Garnet and scheelite as indicators of multi-stage tungsten mineralization in the Huangshaping deposit, southern Hunan province, China. *Ore Geol. Rev.* 94, 193–211. doi:10.1016/j.oregeorev.2018.01.029
- Dong, S. W., Zhang, Y. Q., Long, C. X., Yang, Z. Y., Ji, Q., Wang, T., et al. (2008). Jurassic tectonic revolution in China and new interpretation of the 'yanshan' movement. *Acta Geol. Sin.* 82, 334–347. doi:10.1111/j.1755-6724.2008.tb00583.x
- Duan, Z., Gleeson, S. A., Gao, W. S., Wang, F. Y., and Li, J. W. (2020). Garnet U-Pb dating of the Yinan Au-Cu skarn deposit, Luxi District, North China Craton: Implications for district-wide coeval Au-Cu and Fe skarn mineralization. *Ore Geol. Rev.* 118, 103310–103318. doi:10.1016/j.oregeorev.2020.103310
- Han, F., and Ge, C. H. (1983). Geological and geochemical characteristics of the marine volcanic hydrothermal - sedimentary origin of Makeng iron ore deposit in Fujian Province (in Chinese). *Annu. Rep. Chin. Acad. Geol. Sci.* 8, 154–165.
- Hong, W., Zhang, Z. H., Jiang, Z. S., Li, F. M., and Liu, X. (2012). Magnetite and garnet trace element characteristics from the Chagangnuoer iron deposit in the Western Tianshan Mountains, Xinjiang, NW China: Constrain for ore Genesis (in Chinese with English abstract). *Acta Petrologica Sin.* 28, 2089–2102.
- Lai, S. H., Chen, R. Y., Zhang, D., Di, Y. J., Gong, Y., Yuan, Y., et al. (2014). Petrogeochemical features and zircon LA-ICP-MS U-Pb ages of granite in the Pantian iron ore deposit, Fujian Province and their relationship with mineralization (in Chinese with English abstract). *Acta Petrol. Sin.* 30, 1780–1792.
- Li, D. F., Fu, Y., and Sun, X. M. (2018). Onset and duration of Zn-Pb mineralization in the Talate Pb-Zn (-Fe) skarn deposit, NW China: Constraints from spessartine U-Pb dating. *Gondwana Res.* 63, 117–128. doi:10.1016/j.gr.2018.05.013
- Li, J. H., Zhang, Y. Q., Dong, S. W., and Li, H. L. (2012). Late mesozoic-early cenozoic deformation history of the yuanma basin, central South China. *Tectonophysics* 570–571, 163–183. doi:10.1016/j.tecto.2012.08.012
- Liu, Y. S., Hu, Z. C., Zong, K. Q., Gao, C. G., Chen, H. H., Xu, J., et al. (2010). Reappraisal and refinement of zircon U-Pb isotope and trace element analyses by LA-ICP-MS. *Chin. Sci. Bull.* 55, 1535–1546. doi:10.1007/s11434-010-3052-4
- Ludwig, K. R. (2003). *Isoplot 3.00: A geochronological toolkit for microsoft excel*. California, Berkeley: Berkeley Geochronology Center.
- Seman, S., Stockli, D. F., and Mclean, N. M. (2017). U-Pb geochronology of grossular-andradite garnet. *Chem. Geol.* 460, 106–116. doi:10.1016/j.chemgeo.2017.04.020
- Stifeeva, M., Salnikova, E., Samsonov, A. V., Kotov, A. B., and Gritsenko, Y. D. (2019). Garnet U-Pb age of skarns from dashkesan deposit (lesser caucasus). *Dokl. Earth Sc.* 487, 953–956. doi:10.1134/S1028334X19080178
- Tang, Y. W., Gao, J. F., Lan, T. G., Cui, K., Han, J. J., Zhang, X., et al. (2021). *In situ* low-U garnet U-Pb dating by LA-SF-ICP-MS and its application in constraining the origin of Anji skarn system combined with Ar-Ar dating and Pb isotopes. *Ore Geol. Rev.* 130, 103970–104015. doi:10.1016/j.oregeorev.2020.103970
- Wafforn, S., Seman, S., Kyle, J. R., Stockli, D., Cloos, M., Sonbait, D., et al. (2018). Andradite garnet U-Pb geochronology of the big Gossan skarn, Ertsberg-Grasberg mining district, Indonesia. *Econ. Geol.* 113, 769–778. doi:10.5382/econgeo.2018.4569
- Wang, D. H., Chen, Z. H., Chen, Y. C., and Tan, J. X. (2010). New data of the rock forming and ore-forming chronology for China's important mineral resources areas (in Chinese with English abstract). *Acta Geol. Sin.* 84, 1030–1040.
- Wang, L. J., Wang, J. B., Wang, Y. W., and Shimazaki, H. (2002). REE geochemistry of the Huangguangliang skarn Fe-Sn deposit, Inner Mongolia (in Chinese with English abstract). *Acta Petrol. Sin.* 18, 575–584.
- Wang, S., Zhang, D., Vatuva, A., Yan, P. C., Ma, S., Feng, H. B., et al. (2015). Zircon U-Pb geochronology, geochemistry and Hf isotope compositions and their implications of the dayang and jzhou granites from longyan area in fujian province (in Chinese with English abstract). *Geochemistry* 44, 440–468.
- Wang, S., Zhang, D., Wu, G. G., Cao, K., Qu, H. J., Ma, S., et al. (2017a). New geochronologic evidence of diabases and their metallogenetic relationship with the Makeng-type iron deposits in Southwest Fujian, SE China. *Acta Geol. Sin. - Engl. Ed.* 91, 2324–2326. doi:10.1111/1755-6724.13473
- Wang, S., Zhang, D., Wu, G. G., Vatuva, A., Di, Y. J., Yan, P. C., et al. (2017b). Late Paleozoic to Mesozoic extension in southwestern Fujian Province, South China: Geochemical, geochronological and Hf isotopic constraints from basic-intermediate dykes. *Geosci. Front.* 8, 529–540. doi:10.1016/j.gsf.2016.05.005
- Wang, S., Zhang, D., Wu, G. G., Yi, J. J., and Li, X. J. (2018a). Metallogenetic structural plane characteristics and its prospecting importance for makeng type Fe deposits in southwestern fujian province (in Chinese with English abstract). *J. Geomechanics* 24, 199–211. doi:10.12090/j.issn.1006-6616.2018.24.02.021
- Wang, S., Zhang, D., Yu, T. D., Wu, G. G., Di, Y. J., Zhang, Y. Y., et al. (2021). Geochronology and S-Pb-O-H isotopic constraints on the generation of the Luoyang Fe deposit in southwest Fujian Province, SE China. *Resour. Geol.* 71, 63–79. doi:10.1111/rge.12247.1111/rge.12247
- Wang, S., Zhang, S. H., Zhag, Q. Q., Liang, X., Kong, L. H., Hu, G. H., et al. (2022). *In-situ* zircon U-Pb dating method by LA-ICP-MS and discussions on the effect of different beam spot size on the dating results (in Chinese with English abstract). *J. geomechanics* 28, 642–652. doi:10.12090/j.issn.1006-6616.2021140
- WangZhang, S. D., Wu, G. G., Yi, J. J., Li, X. J., Gao, X. Q., Vatuva, A., et al. (2018b). Late mesozoic tectonic evolution of southwestern fujian province, South China: Constraints from magnetic fabric, zircon U-Pb geochronology and structural deformation. *J. Earth Sci.* 29, 391–407. doi:10.1007/s12583-017-0968-5
- Xing, G. F., Lu, Q. D., Chen, R., Zhang, Z. Y., Nie, T. C., Li, L. M., et al. (2008). Study on the ending time of late mesozoic tectonic regime transition in South China: Comparing to the yanshan area in north China (in Chinese with englis abstract). *Acta Geol. Sin.* 82, 451–463.
- Yan, P. C. (2013). *Discussion the genesis of Makeng iron ore-deposit, Fujian Province (in Chinese with English abstract)*. Beijing: China University of Geosciences, 1–84.

## Publisher's note

All claims expressed in this article are solely those of the authors and do not necessarily represent those of their affiliated organizations, or those of the publisher, the editors and the reviewers. Any product that may be evaluated in this article, or claim that may be made by its manufacturer, is not guaranteed or endorsed by the publisher.

- Yang, F. Q., Mao, J. W., Xu, L. G., Zhang, Y., and Liu, F. (2007). REE geochemistry of the Mengku iron deposit, Xinjiang, and its indication for iron mineralization (in Chinese with English abstract). *Petrol. Sin.* 23, 2443–2456.
- Yang, Y. L., Ni, P., Pan, J. Y., Wang, G. G., and Xu, Y. F. (2017). Constraints on the mineralization processes of the Makeng iron deposit, eastern China: Fluid inclusion, H-O isotope and magnetite trace element analysis. *Ore Geol. Rev.* 88, 791–808. doi:10.1016/j.oregeorev.2016.11.018
- Yu, T. D. (2017). *The "Three-in-One" characteristics and metallogenetic mechanism of Luoyang iron ore in zhangping city, fujian province (in Chinese with English abstract)*. Beijing: China University of Geosciences, 1–70.
- Yuan, Y. (2020). *Petrogenesis of early cretaceous granitoids and Fe-Mo polymetallic mineralization in yongding—dehua area*. Beijing: China University of Geosciences, 1–221.
- Yuan, Y., Zhang, D., Feng, H. B., Di, Y. J., Wang, C. M., and Ni, J. H. (2014). The Re-Os isotope geochronology of Dapai iron polymetallic ore deposit in Yongding County, Fujian Province and its genetic significance. *Acta Geol. Sin. - Engl. Ed.* 88, 1025–1026. doi:10.1111/1755-6724.12378\_30
- Zhang, C. S., Li, L., Zhang, Q. Q., and Wang, J. R. (2012a). LA-ICP-MS zircon U-Pb ages and Hf isotopic compositions of Dayang granite from Longyan, Fujian Province (in Chinese with English abstract). *Geoscience* 26, 433–544.
- Zhang, C. S., Mao, J. W., Zhang, C. Q., and Yu, M. (2013). Fluid inclusion characteristics and metallogenetic mechanism of Makeng skarn Fe-Mo deposit in Fujian Province (in Chinese with English abstract). *Mineral. Deposits* 32, 390–396.
- Zhang, D., Wu, G. G., Di, Y. J., Wang, C. M., and Yao, J. M. (2012b). Geochronology of diagenesis and mineralization of the Luoyang iron deposit in Zhangping city, Fujian province and its geological significance (in Chinese with English abstract). *Earth Sci.* 37, 1217–1231. doi:10.3799/dqkx.2012.130
- Zhang, X. D., Meng, X. H., Chen, Z. X., Wang, J., and Xiu, C. X. (2018a). Comprehensive study of the geological and geophysical characteristics of the metallogenic belt in Southwest Fujian-A case study in the Yongding-Dapai polymetallic ore deposit (in Chinese with English abstract). *Chin. J. Geophys.* 61, 1588–1595. doi:10.6038/cjg2018L0666
- Zhang, Y. Q., Dong, S. W., Li, J. H., Cui, J. J., Shi, W., Su, J., et al. (2012c). The new progress in the study of Mesozoic tectonics of South China (in Chinese with English abstract). *Acta Geol. Sin.* 33 (03), 257–279. doi:10.3975/cagsb.2012.03.01
- Zhang, Z. J., Cheng, Q. M., Yang, J., and Hu, X. L. (2018b). Characterization and origin of granites from the Luoyang Fe deposit, southwestern fujian province, South China. *J. Geochem. Explor.* 184, 119–135. doi:10.1016/j.gexplo.2017.10.015
- Zhang, Z. J., Zuo, R. G., and Cheng, Q. M. (2015). The mineralization age of the makeng Fe deposit, South China: Implications from U-Pb and Sm-Nd geochronology. *Int. J. Earth Sci.* 104, 663–682. doi:10.1007/s00531-014-1096-4
- Zhang, Z. J., and Zuo, R. G. (2014). Sr-Nd-Pb isotope systematics of magnetite: Implications for the Genesis of Makeng Fe deposit, southern China. *Ore Geol. Rev.* 57, 53–60. doi:10.1016/j.oregeorev.2013.09.009
- Zhang, Z., and Zhang, C. S. (2014). Skarn mineral characteristics and zonation of the Makeng Fe-Mo deposit in Fujian Province. *Acta Petrol. Sin.* 30, 1339–1354.
- Zhao, X. L., Yu, S. Y., Yu, M. G., Jiang, Y., and Mao, J. R. (2016). Geological characteristics and metallogenetic epochs of the Dapai Fe-Pb-Zn polymetallic deposit in yongding county, fujian province. *Geol. China* 43, 174–187.